UNIVERSITY OF LEEDS

Investigating the Role of BACE1 in Angiogenesis

Eva Maya Clavane

Submitted in accordance with the requirements for the degree of Master of Science by Research

The University of Leeds

School of Medicine

August 2020

Supervisor: Dr Paul Meakin

Word count: 16,183

The candidate confirms that the work submitted is her own and that appropriate credit has been given where reference has been made to the work of others.

Acknowledgments

Firstly, I would like to thank my primary supervisor, Dr Paul Meakin, for his endless support, advice and guidance throughout my research project and during the Covid-19 pandemic. I would also like to thank my secondary supervisor, Dr Richard Cubbon, for sharing his expertise in the field of angiogenesis and for guiding me through the retinal staining experiment which proved invaluable to this study. Additionally, I would like to thank Jane Brown for her incredible assistance, training and patience regarding laboratory practices and techniques. Lastly, I would like to acknowledge my colleagues and friends at LICAMM for providing an enjoyable and supportive working environment.

Abstract

β-site amyloid precursor protein (APP) cleaving enzyme 1 (BACE1) is a transmembrane aspartyl protease notorious for its contribution to the aetiology of Alzheimer's disease (AD). Notably, BACE1 is elevated in diseases displaying aberrant angiogenesis, including diabetes mellitus (DM), and is implicated in VEGF Receptor 1 (VEGFR1) proteolysis (Devi *et al*., 2012 and Cai *et al.,* 2012). Therefore, we hypothesise that increased BACE1 activity in DM contributes to the altered angiogenesis displayed in associated microvascular complications, including diabetic foot ulcers (DFUs), and that BACE1 inhibitors may prevent such problems.

In vivo observations of the endothelium in the retina of $BACE1^{-/-}$ mice displayed a hyper-branching phenotype in comparison to wild types. This was characterised by a decrease in radial outgrowth but an increase in branch points, percentage vasculature area and quantity of filopodia. This finding was further supported *in vitro* when exploiting the fibrin gel angiogenesis assay. Here, BACE1 inhibition of human umbilical vein endothelial cells (HUVECs) exhibited an increase in sprouting (17 ± 3%, P=<0.001) compared to controls. Lastly, an increase in the phosphorylation of eNOS at Serine 1177 in HUVECs (+ 0.8 ± 0.2, P=0.05) and primary lung endothelial cells (PECs) (+ 0.2 ± 0.02), prior to VEGF stimulations, provided a possible insight into the pro-angiogenic mechanisms of BACE1 inhibition.

Overall, our findings suggest that BACE1 inhibitors, previously trialled to treat AD, could be repurposed to normalise angiogenesis in DM. This may reduce the risk of microvascular complications from developing and prevent consequent amputations.

Key words: Angiogenesis; BACE1; Diabetes Mellitus; Proteolysis; DFUs

Table of Contents

List of Figures

List of Tables

Abbreviations

AD	Alzheimer's disease
ADAM	A-disintegrin and metalloproteinase
AICD	Cytoplasmic amyloid precursor protein intracellular domain
Akt	Protein Kinase B
Ang1/2	Angiopoietin 1/2
ANOVA	Analysis of variance
AP-1	Activator Protein 1
APP	Amyloid precursor protein
Aβ	Amyloid β peptide
BACE1	β-site amyloid precursor protein-cleaving enzyme 1
BSA	Bovine serum albumin
CTF	C-terminus fragment
DAG	Diacylglycerol
DFU	Diabetic foot ulcers
Dll1/4	Delta Like Canonical Notch Ligand 1/4
DM	Diabetes Mellitus
DMSO	Dimethyl sulfoxide
eNOS	Endothelial nitric oxide synthase
F2,6P2	Fructose 2,6-bisphosphate
FGF	Fibroblast growth factor
Flt-1	Vascular endothelial growth factor receptor 1
HIFs	Hypoxia-inducible factor
HUVECs	Human umbilical vein endothelial cells
Jag1/2	Jagged 1/2
KO	Knock-out
M3	β-Secretase Inhibitor IV
MAPK	Mitogen-activated protein kinase
MCP-1	Monocyte Chemoattractant Protein-1

miRNA	Micro- Ribonucleic acid
MMPs	Matrix metallopeptidases
Navβ2	Sodium gated voltage channel β2
NF-κB	Nuclear factor-κB
NICD1	Notch Intracellular Domain 1
NO	Nitric oxide
NOX	NADPH-oxidase
Nrg1	Neuregulin 1
P3	3Kda peptide
PAD	Peripheral Arterial Disease
PAGE	Polyacrylamide gel electrophoresis
PBS	Phosphate buffered saline
PDGF	Platelet-derived growth factor
PECs	Pulmonary endothelial cells
PFK-1	Phosphofructokinase-1
PFKFB3	6-phosphofructo-2-kinase/fructose-2,6-biphosphatase 3
PKC	Protein Kinase C
ROS	Reactive Oxygen Species
RTKs	Receptor Tyrosine Kinases
SDS	Sodium dodecyl sulphate
sFlt-1	Soluble fms-like tyrosine kinase
SPRY2	Sprouty homolog 2
STAT3	Signal transducer and activator of transcription 3
SVECs	Saphenous vein endothelial cells
TBS	Tris-buffered-saline
TBST	Tris-buffered-saline-Tween®-20
TGF-β	Transforming growth factor β
VEGF	Vascular endothelial growth factor
VEGFR	Vascular endothelial growth factor receptor
WT	Wild type

1. Introduction

1.1 Diabetes Mellitus

Diabetes Mellitus (DM), commonly known as diabetes, is a chronic metabolic and inflammatory disease. Although it currently effects approximately half a billion people globally, this statistic is predicted to increase rapidly in the coming years (Saeedi *et al.*, 2019). DM has two major forms: type 1 and type 2, resulting from defective insulin production or insulin insensitivity, respectively. However, both types lead to elevated blood glucose levels, a condition defined as hyperglycaemia (Tan *et al*., 2019).

Insulin is a vital anabolic peptide hormone secreted by β cells of the pancreatic islets of Langerhans (Wilcox, 2005). Its role involves maintaining normal blood glucose levels, regulating metabolism of carbohydrates, lipids and proteins and stimulating cell growth and division. Duvillié *et al* showed insulin deficient mice pups were growth retarded, instantly developed DM with a build-up of toxic ketones in the blood (ketoacidosis) and died within 48 hours (Duvillié *et al*., 1997). This demonstrates the important physiological role of insulin signalling in health and disease and the implications which may arise in poorly controlled DM.

1.1.2 Diabetes and peripheral complications

In England, individuals with DM are 23 times more likely to suffer a lower limb amputation than people without DM (NICE, 2015 and Holman, Young & Jeffcoate, 2012). Not only does this have devastating socioeconomic consequences, but it is an encumbrance on the National Health Service (NHS), consuming between £837 million and £962 million; 0.8% to 0.9% of the NHS budget in 2014-2015 (Kerr *et al*., 2019). Of the individuals with DM that endure a lower limb amputation, 84% are attributed to diabetic foot ulceration (DFU). This common complication found in 10% of diabetics is characterised by painful sores and disintegration of dermal tissues which are prone to infection

(Pecoraro, Reiber & Burgess, 1990; NICE, 2015; Okonkwo & DiPietro, 2017). Therefore, prevention of DFUs is recognised as the most appropriate way to avoid amputations (Reekers and Lammers., 2012). Furthermore, the mortality rate five-years post-amputation is a considerable 50-59 %, confirming that DFUs are one of the most devastating complications of DM (Martins-Mendes *et al*., 2014).

There are numerous factors which contribute to DFUs, with diabetic neuropathy and peripheral arterial disease (PAD) being the most important (Pendsey, 2010). PAD is a chronic manifestation of atherosclerotic plaques in peripheral arteries, which leads to occlusion of the vessels and decreased blood flow to limbs (Ouriel, 2001 and Clegg, 2017). Despite the shortage of oxygen in surrounding tissues (ischaemia) which acts as a potent pro-angiogenic stimulus, angiogenesis is defective in many individuals with DM suffering with PAD due to the unfavourable cellular environment it produces (Clegg, 2017). Moreover, DFUs are worsened by concomitant diabetic neuropathy. Diminished sensory feedback and perceived pain in the individual, prevents them from seeking medical intervention (Thiruvoipati, Kielhorn & Armstrong, 2015).

Treatments for PAD are heavily reliant on surgery. These include either open bypass surgery using an autologous vein or prosthetic graft, or endovascular techniques using various devices to widen the arterial lumen (Kota *et al*., 2013). Although these are successful procedures in improving perfusion, they are extremely invasive and insufficient in preventing DFUs. (Perez-Favila *et al*., 2019). This is because there are additional cellular and molecular factors in DM preventing sufficient revascularisation.

Currently, there is not an exclusive treatment for DFU's; the seriousness of the condition is monitored by specialists to prevent infection. To reduce the chances of a problematic DFUs, DM patients are encouraged to off-load the pressure placed on the wound, pursue debridement procedures and protect wounds with suitable treatments and dressings (APMA, 2020). These measures are accompanied by the individual effectively managing their blood glucose levels to

prevent additional complications. This study will explore whether BACE1 inhibiting drugs, previously investigated in clinical trials for treating early ons*et* Alzheimer's Disease (AD), can be repurposed to improve revascularization of DFUs.

1.2 Angiogenesis

The cardiovascular system is comprised of the heart, blood and a vast network of tubular vessels (Chung, Lee & Ferrara, 2010). It is involved in transporting oxygenated blood, nutrients, hormones and immune cells to tissues and organs, and the disposal of their waste metabolites. Oxygenated blood originating from the heart is pumped through a large vessel, known as an artery, which subsequently disperses and reduces in diameter to arterioles and eventually capillaries (Okonkwo & DiPietro, 2017). Capillaries are extremely abundant, ensuring each cell is within 100-200 microns of a blood supply (Okonkwo & DiPietro, 2017). Furthermore, their anatomy consists of a singular layer of endothelium with a diameter around 8–20 microns which assists in rapid reciprocal diffusion of substances (Pittman, 2011).

The extensive vascular tree established in adults is the product of the two processes, vasculogenesis and angiogenesis. Vasculature is initially formed in the embryo by vasculogenesis; a *de novo* process requiring precursor cells (angioblasts) to differentiate into endothelial cells and form a primary capillary plexus (Swift & Weinstein, 2009 and Risau, 1997). The framework of primitive vessels produced by vasculogenesis is subsequently exploited by angiogenesis, defined as the growth of blood vessels from pre-existing ones, which substantially expands the vasculature network (Swift & Weinstein, 2009). Although the two processes predominately occur during growth and development, angiogenesis is utilised throughout adulthood for processes such as wound healing, menstruation and pregnancy (Vailhé, Vittet & Feige, J., 2001). In these situations, an additional demand for nutrients and oxygen causes existing vascular networks to become pro-angiogenic and produce branches of new vessels. Nascent vessels orientate their growth towards the starving tissue

before fusing with existing vasculature and establishing a functional circuit (Blanco & Gerhardt, 2013). Once the demand of nutrients and oxygen are met, the vessel reverts to a quiescent state where the capillaries are enveloped by pericytes, a mural cell embedded in the basement membrane (Shepro & Morel, 1993).

1.2.1 Cellular and molecular mechanisms of angiogenesis

Angiogenesis is a reactionary and complex multistep process (Potente & Carmeliet, 2017). At a cellular level, endothelial cells 'sprout' from a selected position of an existing vessel before proliferating and trailing towards environmental cues, all whilst maintaining contact with the parent vessel (Betz *et al*., 2016).

1.2.1.1 Angiogenesis initiation

Oxygen-deficient (hypoxic) cells trigger angiogenesis by signalling through hypoxia-inducible transcription factors (HIFs) (Carmeliet, 2003). HIFs upregulate numerous angiogenic genes including FGF, Angiopoietins, PDGF, MCP-1, TGF, various integrins, VE-cadherin, ephrins, nitric oxide, but most importantly VEGF-A (henceforth VEGF). VEGF belongs to a family of cysteine knot proteins and is a potent angiogenic factor which activates quiescent endothelial cells (Woolard *et al*., 2009). It signals through auto and paracrine mechanisms by binding to homologous Receptor Tyrosine Kinases (RTKs), including VEGF Receptor 2 (VEGFR2), to stimulate proliferation, migration and phenotypic differentiation through its major intracellular phosphorylation sites Y1175 and Y1214 (Laurent, Fabrice & Jacques, 2007).

1.2.1.2 Tip cell selection

Angiogenesis commences with the selection and differentiation of endothelial cells to either a tip or stalk cell phenotype (Blanco & Gerhardt, 2013). Tip cells are migratory endothelial cells selected to guide the angiogenic sprout formation towards an area of hypoxia. They are abundant in long and dynamic filopodial extensions which pave the way for the nascent sprout. Contrastingly, stalk cells which have fewer filopodia and are highly proliferative trail behind the tip cell elongating the vessel and forming its lumen (Geudens & Gerhardt, 2011). Tip and stalk cell phenotypes are the product of reciprocal VEGF and NOTCH signalling.

Aforementioned, hypoxic cells generate VEGF which produces a chemical gradient. Once the VEGF reaches a quiescent vessel, it binds to VEGFR2 on endothelial cells and, through intracellular signalling, instructs it to adopt a tip cell phenotype (Blanco & Gerhardt, 2013). To prevent over production of sprouts, tip cells laterally inhibit neighbouring cells from acquiring this phenotype through Dll4/NOTCH1 signalling, ensuring network formation (Lobov *et al.,* 2007).

Endothelial cells express NOTCH1 and NOTCH4 receptors, as well as their ligands Delta-like 1 (Dll1), Delta-like 4 (Dll4), Jagged-1 (Jag1) and Jagged-2 (Jag2) (Roca & Adams, 2007). To engage in lateral inhibition, Dll4 ligands expressed on tip cells bind and activate NOTCH1 receptors on neighbouring cells (Figure 1). Once activated, the NOTCH1 receptor is proteolytically cleaved by proteases of the ADAM family, releasing a NOTCH1 intracellular domain (NICD1) (Nichols *et al*., 2007). The NICD1 transports to the nucleus where it down-regulates VEGFR2 expression and upregulates Dll4, Jag1 and VEGF Receptor 1 (VEGFR1) expression, characteristic of stalk cells (Geudens & Gerhardt, 2011 and Harrington *et al.,* 2008). VEGFR1 receptors act to down-regulate VEGF signalling by binding to it with a much higher affinity and possessing a weaker tyrosine kinase activity (Shibuya., 2011). Therefore, reduced VEGF signalling in these cells prevent tip cell differentiation (Potente & Carmeliet, 2017). Moreover, increased Jag1 expression in stalk cells down-regulates Dll4/NOTCH1 signalling by competing for the NOTCH1 active site (Benedito *et al*., 2009; and Nichols *et al*., 2007).

Once Jag1 binds NOTCH1, it transduces a much weaker signal, preventing stalk cells from activating NOTCH1 signalling and subsequent gene expression in neighbouring tip cells (Benedito *et al*., 2009).

The phenotypic differentiation of tip and stalk cells regulated by VEGF and NOTCH1 signalling is dynamic. Time-lapse microscopy imaging of angiogenic sprouts has identified the ability of phenotypic switching between tip and stalk states (Nichols *et al*., 2007). This presents the versatile nature of blood vessels, as their phenotype is constantly being re-evaluated to allow the vessel to adapt accordingly to environmental cues.

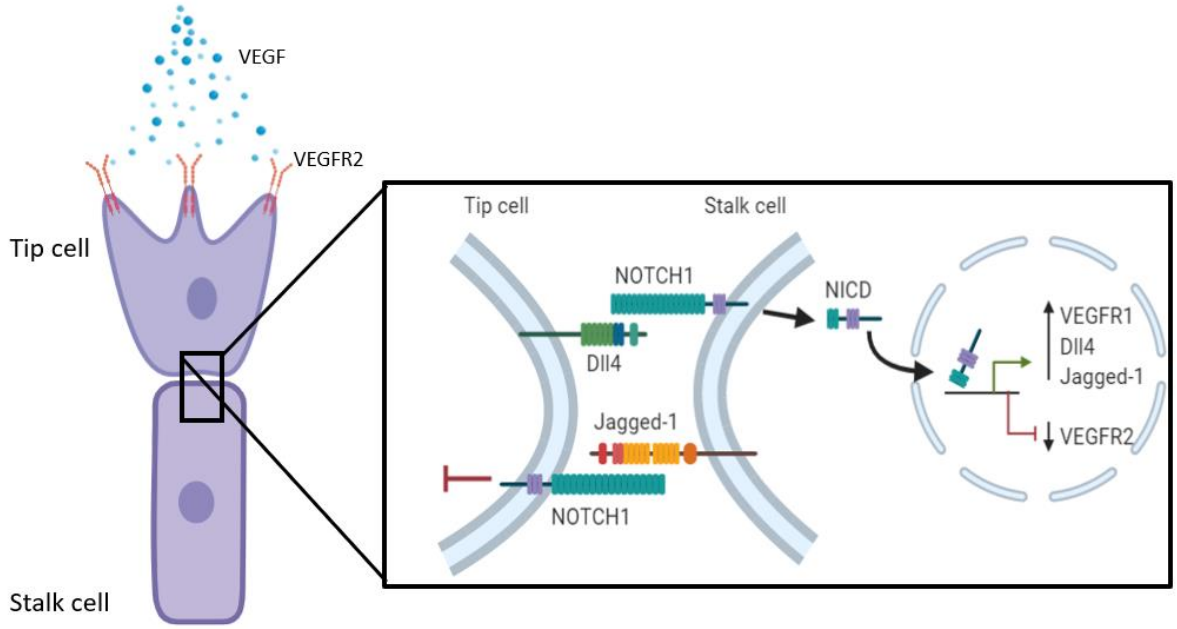

Figure 1: A schematic diagram presenting the effects of NOTCH1 signalling in both tip and stalk cells. Stalk cells predominately express NOTCH1 receptors which bind to Dll4, a ligand predominately expressed on tip cells. Dll4/NOTCH1 signalling releases NICD1 which initiates a downstream cascade within the stalk cells, allowing it to retain its phenotype. To prevent such signalling in tip cells from occurring, Jag1 is expressed widely on stalk cells. Jag1/NOTCH1 transduces a weaker signal, preventing NICD1 signalling occurring in neighbouring tip cells (adapted from Siemerink *et al*., 2013).

Independent of NOTCH signalling, metabolic pathways including 6-phosphofructo-2-kinase/fructose-2,6-bisphosphatase-3 (PFKFB3) -driven glycolysis are also responsible for determining tip cell

selection (Figure 2) (Sawada & Arany, 2017). VEGFR2 signalling increases glycolysis by two-fold via upregulating the expression of a potent glycolytic activator, PFKFB3 (De Bock *et al*., 2013). PFKFB3 generates fructose-2,6-bisphosphate (F2,6P2) which is an allosteric activator of phosphofructokinase-1 (PFK-1). PFK-1 is a transferase responsible for converting fructose 6-phosphate and ATP to fructose 1,6-bisphosphate and ADP. Therefore, the glycolytic flux induced by VEGFR2-induced glycolysis, overrides Dll4/NOTCH1 signals and encourages a tip cell formation. Moreover, stalk cells exhibit diminished VEGFR2 signalling and have reduced glycolysis, which cannot counteract NICD1 signals (Stapor *et al*., 2014). Inhibition of PFK-1 and the subsequent reduction of glycolysis in endothelial cells was found to be detrimental to vascular angiogenic potential, impeding sprouting, migration and proliferation processes (De Bock *et al*., 2013). Therefore, upregulation of PFKFB3 by VEGFR2 signalling at the vascular front further encourages tip cell characteristics.

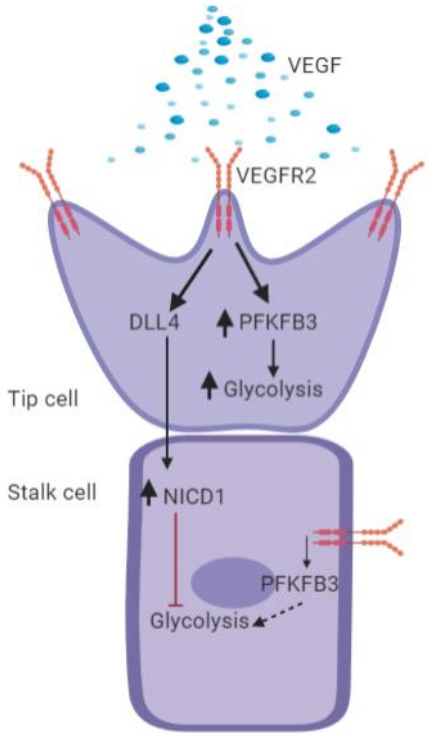

Figure 2: A schematic diagram presenting the influences of glycolysis in tip cell determination. Tip cells have increased VEGFR2 signalling resulting in increased PFKFB3 expression and glycolysis which determines the tip cell phenotype. Contrastingly, stalk cells have reduced PFKFB3 and glycolysis which is further undermined by NICD1 signalling (adapted from Stapor *et al.,* 2014).

1.2.1.3 Extracellular matrix degradation

The vasculature is supported by a highly specialised extracellular matrix, known as the basement membrane, which consists of collagen IV, laminins, entactin, and heparan sulfate proteoglycans (Neve *et al*., 2014). Prior to angiogenesis, it is essential that the basement membrane is broken down to assist tip cell migration; a procedure which is stimulated by VEGF binding to VEGFR2 (Lamalice *et al.,* 2004). VEGFR2 activation upregulates angiopoietin-2 (Ang-2) expression, a growth factor which binds to an autocrine receptor (Tie-2), interfering with the angiopoietin-1/Tie-2 signalling pathway (Oh *et al.,* 1999). This pathway aids cellular migration by relieving inter-endothelial contacts through upregulating various matrix metalloproteinases (MMPs). MMPs detach endothelial cells from smooth muscle cells and the underlying basement membrane, permitting angiogenesis (Conway, Collen & Carmeliet, 2001).

1.2.1.4 Sprout formation

Through numerous downstream signalling pathways, VEGFR2 activation assists in endothelial migration and proliferation, resulting in the formation of a nascent sprout (Figure 3).

Firstly, VEGFR2 signalling triggers endothelial migration by activating numerous GTPases such as Cdc42 and Rac1 (Laurent, Fabrice & Jacques, 2007). Activated Cdc42 and Rac1 generate structures, such as stress fibres and lamellipodia, which are essential in guiding the endothelial cells towards the VEGF gradient to the site of hypoxia (Lamalice *et al.,* 2004).

Additionally, VEGF-mediated migration is initiated through the downstream PI3k/Akt pathway. Akt directly phosphorylates nitric oxide synthase (eNOS) at Ser1177 to induce the production of nitric oxide (NO) (Cooke & Losordo, 2002). Moreover, VEGF dissociates eNOS from a negative regulator-caveolin-1- in endothelial cells, further contributing to NO production (Labrecque *et al*., 2002). NO is a mediator of vasodilation and increases vascular permeability, two processes important in early

stages of angiogenesis. Vasodilation expands the vessel surface, improving responses to angiogenic signals; whereas enhanced vascular permeability facilitates plasma protein extravasation, producing a temporary 'track' for tip cells to migrate along (Eliceiri *et al*., 1999).

Lastly, alongside numerous other pathways, NO is important in cell survival, cell proliferation and the reformation of the basement membrane, further aiding sprout development (Rüegg *et al.,* 1998 and Cooke & Losordo, 2002). Overall, eNOS plays an essential role in angiogenic sprout formation, a concept which is further supported by studies whom discovered that eNOS or NO inhibition attenuates angiogenic responses (Ziche & Morbidelli, 2000 and Ziche *et al.,* 1994).

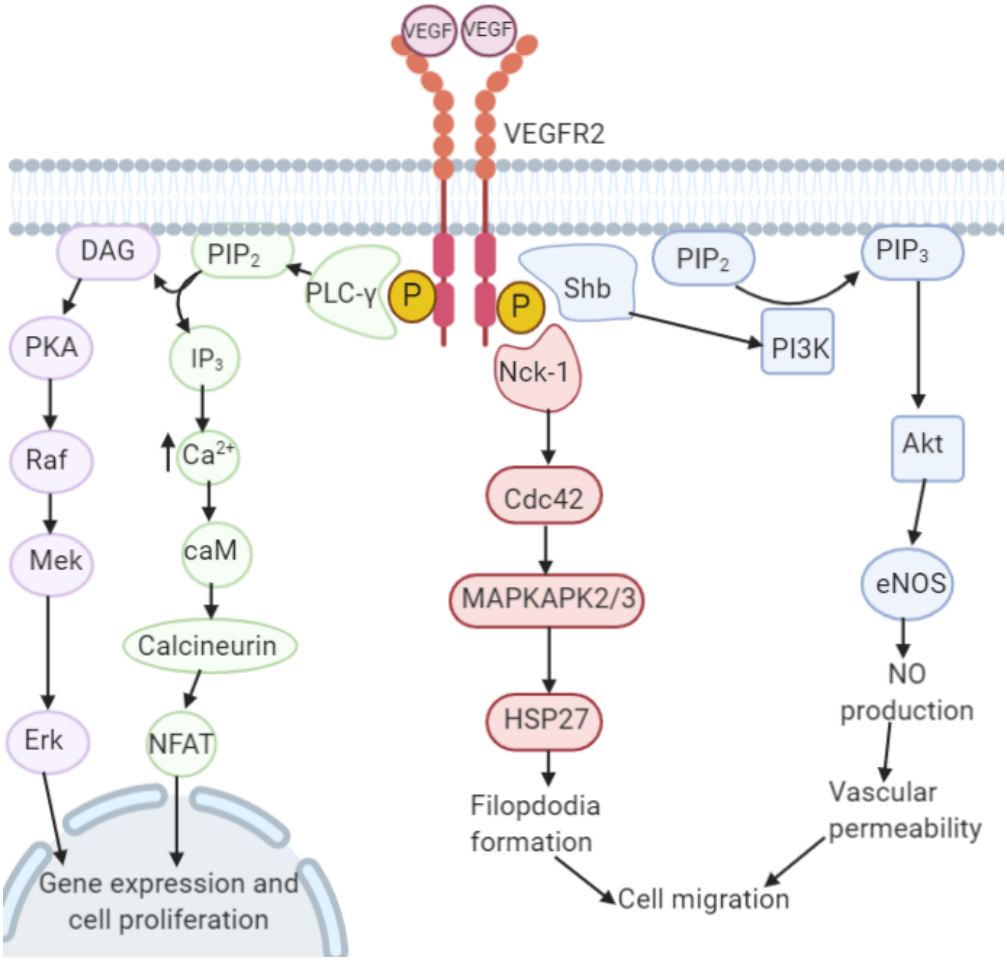

Figure 3: A schematic diagram displaying the pro-angiogenic downstream signalling pathways of VEGFR2. Phosphorylation of the VEGFR2 intracellular domain elicits numerous signals, some of which are dipicted here. These pathways contribute to endothelial cell migration (red and blue) and proliferation (purple and green) which are essential for angiogenic sprout formation (adapted from Matsumoto & Claesson-Welsh, 2001).

1.2.1.5 Vessel maturation

Nascent vessels must undergo several modifications at both a cellular and molecular level to become competent mature vessels.

At a cellular level, the tip cell from a nascent vessel fuses with other vessels through anastomosis to establish a functional vascular circuit. Simultaneously, its phenotype re-establishes an immobile and non-proliferative quiescent state, also referred to as a 'phalanx' cell (Zuazo-Gaztelu & Casanovas, 2018). The capillary network is further refined through controlled cell death, known as apoptosis, to produce an appropriate branching hierarchy (Okonkwo & DiPietro, 2017). Lastly, the vessel is stabilised through the recruitment of pericytes and the recuperation of connections with the basement membrane.

At a molecular level, vessel maturation results from the co-operation of multiple signalling factors, including Angiopoetin-1 (Ang-1), platelet derived growth factor (PDGF), pigment epithelium derived factor (PEDF) and sprouty-2 (SPRY2) (Raica & Cimpean, 2010 and Okonkwo & DiPietro, 2017). Unlike the pro-angiogenic aptitude of Ang-2, Ang-1 is a potent maturation factor which antagonistically binds to Tie-2 to stabilise inter-endothelial and endothelial- perivascular connections. This role has been demonstrated in a study which shows that topical application of Ang-1 neutralising antibodies to diabetic mice models prevents the neovascular maturation process (Li *et al*., 2015).

Moreover, PDGF is a potent anti-angiogenic factor which is constitutively expressed by endothelial cells to maintain homeostasis through apoptosis and reduced vessel permeability (Broadhead *et al*., 2010). Following angiogenic sprout formation, endothelial cells renew PDGF expression. The factor binds to pericytes expressing its complimentary receptor (PDGFR) and recruits them to the maturing vessel to induce stability (Broadhead *et al*., 2010).

Lastly, to revert the vessel to a quiescent state, endothelial cells express SPRY2 which downregulates VEGF-mediated endothelial proliferation by inhibiting downstream mitogen-activated protein kinases (MAPK) pathways (Wietecha *et al*., 2011).

Amongst other signalling cascades, these factors assist in producing fully mature and stable vessels (Zuazo-Gaztelu & Casanovas, 2018). Maturation is an essential stage of angiogenesis which must be fully achieved to allow effective blood perfusion to restore tissue oxygenation.

1.3 Aberrant angiogenesis in DM

Microvascular complications associated with DM can be caused by either excessive or deficient angiogenesis. This report will highlight a selection of factors that contribute to insufficient angiogenesis observed in DFUs (Figure 4), a less understood pathophysiology compared to diabetic retinopathy and nephropathy. Previous research has shown that DFUs have a delayed healing response and decreased capillary density, with 70% of a wound remaining unhealed after 20-weeks of standard treatment (Dinh & Veves, 2005 and Mirza & Koh, 2011). Therefore, to discover an effective treatment to improve vascularisation in DFUs, it is important to understand the defective mechanisms existing here.

Studies investigating wound healing in diabetes are regularly performed in diabetic mice models; in particular, the genetic db/db mouse which has a mutation in the leptin receptor. This mutation produces obese mice displaying hyperlipidaemia, hyperphagia, hyperinsulinemia and hyperglycaemia, which are prominent in humans with type 2 DM (Kobayashi at al., 2000 and Coleman, 1978).

1.3.1 Macrophage activity

During would healing, macrophages switch from a pro-inflammatory phenotype to a pro-reparative phenotype which is essential for supporting tissue regrowth and angiogenesis through their production of VEGF (Okonkwo & DiPietro, 2017). However, in a db/db model, macrophages are less prevalent and resist switching, causing delayed wound healing (Michaels *et al*., 2007).

Since macrophages are an important source of VEGF in wounds, their scarcity could be linked to the poor angiogenic potential seen in those with diabetes (Coleman, 1978). Moreover, reduced phagocytosis of apoptotic cells (efferocytosis) further delays healing, contributing to the chronic wounds presented as DFUs.

1.3.2 Reactive Oxygen Species

Endothelial cells and vascular smooth muscle cells produce low levels of reactive oxygen species (ROS) which are required for physiological processes such as promoting endothelial proliferation during angiogenesis (Kolluru, Bir & Kevil, 2012 and Ushio-Fukai *et al*., 2002). In DM, an imbalance of ROS, termed oxidative stress, leads to aberrant angiogenesis and poor wound healing in DFUs.

Prolonged hyperglycaemia in DM produces advanced glycation end products (AGEs) which are formed by non-enzymatic glycation events (Ramasamy, Yan & Schmidt, 2011). AGEs bind to their complementary receptor, RAGE, which activates the diacylglycerol (DAG)—protein kinase C (PKC)—and NADPH-oxidase (NOX) metabolic pathway, substantially increasing ROS production (Volpe *et al*., 2018). NOXs are transmembrane enzymes which generate ROS (superoxide) by electron transfer from NADPH to molecular oxygen. Once synthesised, ROS can proceed to inactivate and sequester proangiogenic NO, consequently inhibiting angiogenesis (Kolluru, Bir & Kevil, 2012). Moreover, together with hyperglycaemia and AGES, excessive ROS initiates endothelial and pericyte apoptosis through activating transcription factors NF-κB and p21-ras (Chuang *et al*., 2007 and Stern *et al*.,

2002). This prevents vessel proliferation and maturation, consequently preventing sufficient vessel growth in individuals with DM.

1.3.3 Insulin resistance

Insulin resistance, defined as a diminished cellular functional and signalling response to insulin, contributes profoundly to the aetiology of type 2 DM (Wilcox, 2005). The pleotropic effects of insulin signalling in endothelial cells and pericytes are key for all stages of angiogenesis.

Firstly, insulin binding to the insulin receptor upregulates VEGF expression and subsequent VEGF signalling (Yamagishi *et al*., 1999). This was demonstrated by Yamagishi *et al* who found that VEGF monoclonal antibodies could completely neutralise endothelial migration and proliferation in cells induced by insulin.

Secondly, insulin receptor phosphorylation initiates two key pro-angiogenic signalling pathway; PI3K/Akt and MAPK (Escudero *et al*., 2017). Both pathways crosstalk and are valuable in the NO synthesis through increasing L-arginine uptake into endothelial cells and activation of eNOS (Muniyappa *et al*., 2007). The MAPK pathway also mediates cellular proliferation during vessel growth (Escudero *et al*., 2017). Lastly, King *et al* discovered that Insulin induced glucose uptake and proliferation of retinal pericytes which encourages vascular stability (King *et al*., 1983).

To conclude, insulin signalling is a significant pro-angiogenic factor. Therefore, it is unsurprising that insulin resistance contributes to aberrant angiogenesis and microvascular complications visible in DM.

1.3.4 Reduced VEGF signalling

Reports regarding VEGF levels in individuals with DM are conflicting. Surprisingly, many studies have published that individuals with DM have increased circulating VEGF levels (Chen *et al*., 2018). Although this is plausible for explaining diabetic retinopathy and nephropathy, it is difficult to comprehend how an increase in a potent pro-angiogenic factor can cause such deficiency in angiogenic potential in peripheral vasculature. However, researchers have discovered that in clinical PAD, the anti-angiogenic VEGF-A isoform, VEGF-A^{165b}, was particularly upregulated (Kikuchi *et al*., 2014). Additionally, increased visceral fat, prominent in type 2 diabetics, also upregulates this splice variant (Ngo *et al*., 2014). Therefore, the increase of VEGF-A^{165b} in DM can help explain such conundrum.

Moreover, Chen *et al* discovered that diabetics with concomitant DFUs had decreased circulating VEGF in comparison to diabetics without DFUs (Chen *et al*., 2018). In support of this finding, Seitz *et al* found that VEGF protein and miRNA concentrations were reduced in endothelial cells within peripheral wounds of db/db mice (Seitz *et al.*, 2010).

Furthermore, multiple researchers have discovered that topical application of VEGF accelerated wound closure in diabetics, suggesting that poor would healing in DFU could be due to localised VEGF deficiency (Galiano *et al*., 2004., Hanft *et al*., 2008 and Barrientos *et al*., 2014).

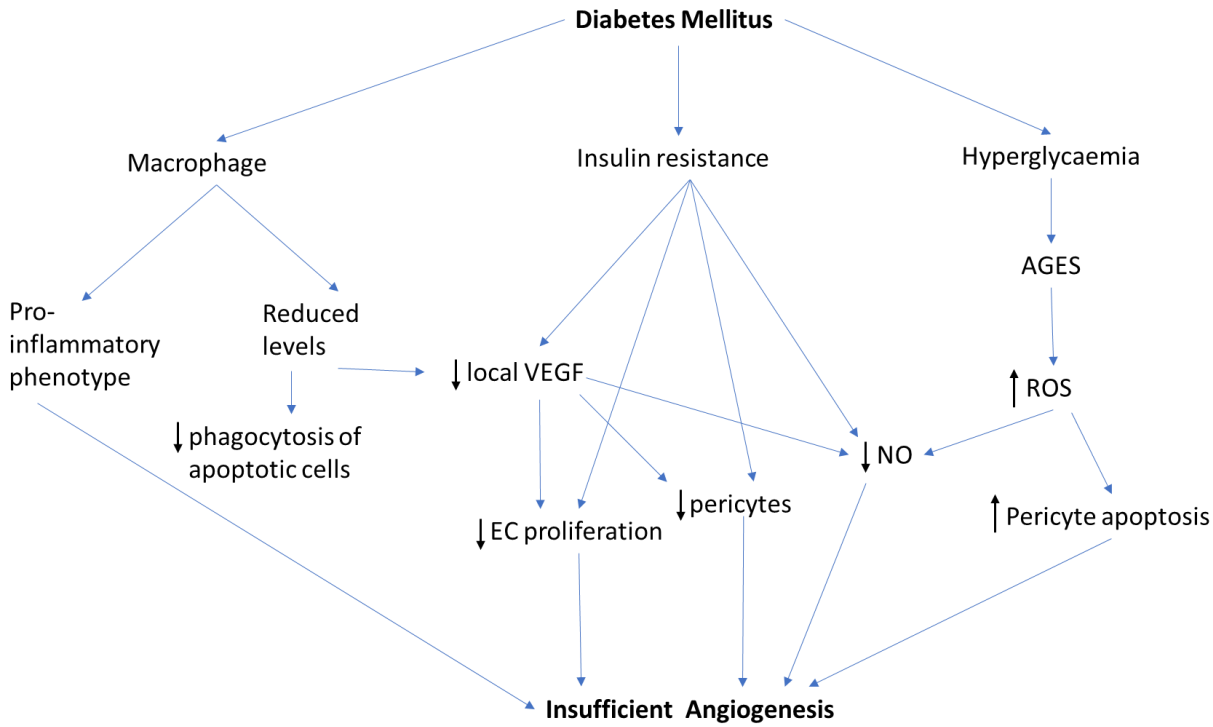

Figure 4: A flow diagram presenting how various factors of DM contribute to insufficient angiogenesis.

Scarce and pro-inflammatory macrophages, insulin resistance and hyperglycaemia are merely three factors of DM which result in insufficient angiogenesis.

Crucially, it must be acknowledged that multiple factors of DM contribute to a reduction in angiogenic potential, and they should all be considered when treating each individual case of DFU. Individuals with DM may suffer from varying degrees of inflammation and cytotoxicity depending on their type and management quality of their DM. Consequently, there may not be one universal treatment for DFUs, suggesting a more 'personal medicine' approach may be more beneficial depending on individual circumstances and severity. Aforementioned, our study aims to determine whether increased BACE1 activity is a factor contributing to aberrant angiogenesis in diabetic models and whether BACE1 inhibitors can restore angiogenic potential.

1.3.4.1 Current VEGF treatments being explored

Building on from the knowledge acquired regarding aberrant angiogenesis in DM wounds and ulcers, various researchers have exposed potential treatments to improve cellular and molecular signalling required for sufficient angiogenesis (Patel *et al*., 2019). Pertinent to this project, scientists have explored ways to increase VEGF levels in VEGF-deficient diabetic wounds to improve angiogenic potential. Regrettably, numerous undesirable effects have arisen when doing so, including retarded blood vessel growth, hemangioma formation and lower extremity oedema (Lee *et al*., 2000 and Baumgartner *et al*., 1998). Furthermore, the half-life of VEGF is very short, and its degradation is extremely rapid; causing difficulties in increasing local VEGF levels topically (Yan *et al.,* 2010). Consequently, this project aims to determine whether BACE1 inhibition prevents a reduction in VEGF bioavailability, allowing sufficient VEGFR2 signalling and angiogenesis to occur in diabetic models.

Chereddy *et al* has attempted to overcome the boundaries of VEGF treatment by encapsulating VEGF in poly lactic-co-glycolic acid (PLGA) nanoparticles (Chereddy *et al*., 2015). The polymer is particularly useful as it has an ideal biocompatibility, biodegradability and high safety profile. Moreover, PLGA supplies lactate to the wound which accelerates angiogenesis and promotes wound healing. Fortunately, PLGA-VEGF treated non-diabetic and diabetic mice displayed a significantly faster wound closure than other experimental groups. Therefore, this research supports the concept that VEGF restoration is sufficient to improve revascularisation and prevent DFU occurrence.

1.4 BACE1

Beta Amyloid Precursor Protein (APP) Cleaving Enzyme 1 (BACE1) is an aspartyl protease first identified in 1999 by multiple research groups (Sinha *et al*., 1999; Vassar *et al*., 1999; Hussain *et al*., 1999; Yan *et al*., 1999; Lin *et al*., 2000). It belongs to a ubiquitous family of pepsin and retroviral

aspartic proteases which are known to catalyse the hydrolytic cleavage of ~80 proteins involved in multiple cellular pathways (Barman & Prabhakar, 2014).

BACE1 is widely expressed, featuring in many cell types, but being most prominent in brain and pancreatic tissue (Dislich & Lichtenthaler, 2012 and Vasser *et al*., 1999). Furthermore, pertinent to this project, research has shown that BACE1 is sufficiently expressed in endothelial cells (Devraj *et al*., 2016 and Meakin *et al*., 2015).

1.4.1 Structure of BACE1

BACE1 is a globular protein consisting of 501 amino acids, 434 of which comprise of the large N-terminal luminal ectodomain. The remaining amino acids contribute to the type-1 transmembrane domain and the short C-terminal tail (Figure 5) (Sathya *et al*., 2012; Benjannet *et al*., 2001; Dislich & Lichtenthaler, 2012). Within its primary and tertiary structures, BACE1 contains a number of notable features which will be highlighted below (Figure 5A).

Firstly, at its N-terminus, BACE1 has a prodomain consisting of a signal sequence (residues 1-21) and a pro-peptide (residues 22-45). The N-terminal domain is key in the initial tertiary folding of BACE1 as well as its exit from the endoplasmic reticulum (ER) (Sathya *et al*., 2012). Furin-like proteases eventually remove the prodomain, granting the mature form of BACE1 to commence at residue Glu46 (Bennett *et al*., 2000).

Following the N-terminal domain is a luminal catalytic domain expanse. Like other β-secretases, BACE1 contains two aspartic protease active site motifs, DTGS (residues 93-96) and DSGT (residues 289-292). Unsurprisingly, a mutation in either conserved aspartic acid residue (D) causes the enzyme to become inactive (Bennett *et al*., 2000). The tertiary structure of the catalytic domain, which resembles a 2-fold symmetry, is held together by six cysteine residues that form three

intramolecular disulphide bonds and several N-linked glycosylation sites (Figure 5B) (Cole and Vassar., 2007).

Furthermore, an antiparallel hairpin loop structure, known as the 'flap', resides in the catalytic domain (residues 67-77), partially shielding the active site (Hong *et al*., 2000; and Dislich & Lichtenthaler, 2012 and Shimizu *et al*., 2008). Conformational changes in the flap permit substrate accessibility and geometric positioning, aiding in proteolysis (Hong *et al*., 2000; Xu *et al*., 2012; Shimizu *et al*., 2008). Water molecules, Wat1 and Wat2, which exist within the active site, stabilise the flap through hydrogen bonding and assist in the hydrolytic cleavage of peptide bonds (Shimizu *et al*., 2008; Andreeva & Rumsh, 2001; and Barman & Prabhakar, 2014). For example, as a substrate enters the active site, hydrogen bonds keeping the flap in an accessible and open confirmation are broken, causing the flap to close and proteolysis to occur (Hong & Tang, 2004 and Ghosh & Osswald, 2014).

Proximal to the C-terminus is a unique single pass transmembrane domain (residues 455-580), which is important in subcellular localisation and enzymatic activity (Harris & Fahrenholz, 2005). This is supported by Yan *et al*., who found that transmembrane domain is critical for BACE1 activity *in vivo*. (Yan *et al*., 2001). Although this structure is not depicted in any of the crystal structures deposited in the protein data bank (PDB) (Figure 5C), the TMHMM bioinformatic tool clearly presents a single-pass transmembrane domain proximal to C-terminus (Figure 5D).

Lastly, at the very C-terminus is a palmitoylated cytoplasmic tail containing a DISLL motif (496-500). The DISLL motif is an acid cluster-dileucine motif (ACDL) involved in endosomal trafficking. In experiments where the motif is deleted or mutated, a greater proportion of BACE1 is localised in the plasma membrane rather than endosomes (Cole and Vassar, 2007). Palmitoylation of the cytoplasmic tail influences protein trafficking and localisation of the mature enzyme through the secretory pathway, particularly to lipid rafts (Sathya *et al*., 2012).

Extensive post-translational modifications cause BACE1 to be constantly cycled between compartments of the secretory pathway (Shimizu *et al.*, 2008). Although BACE1 can be found on the neutral plasma membrane, its optimal activity is within acidic endosomes with a pH 4.5 (Sathya *et al.*, 2012 and Shimizu *et al.*, 2008).

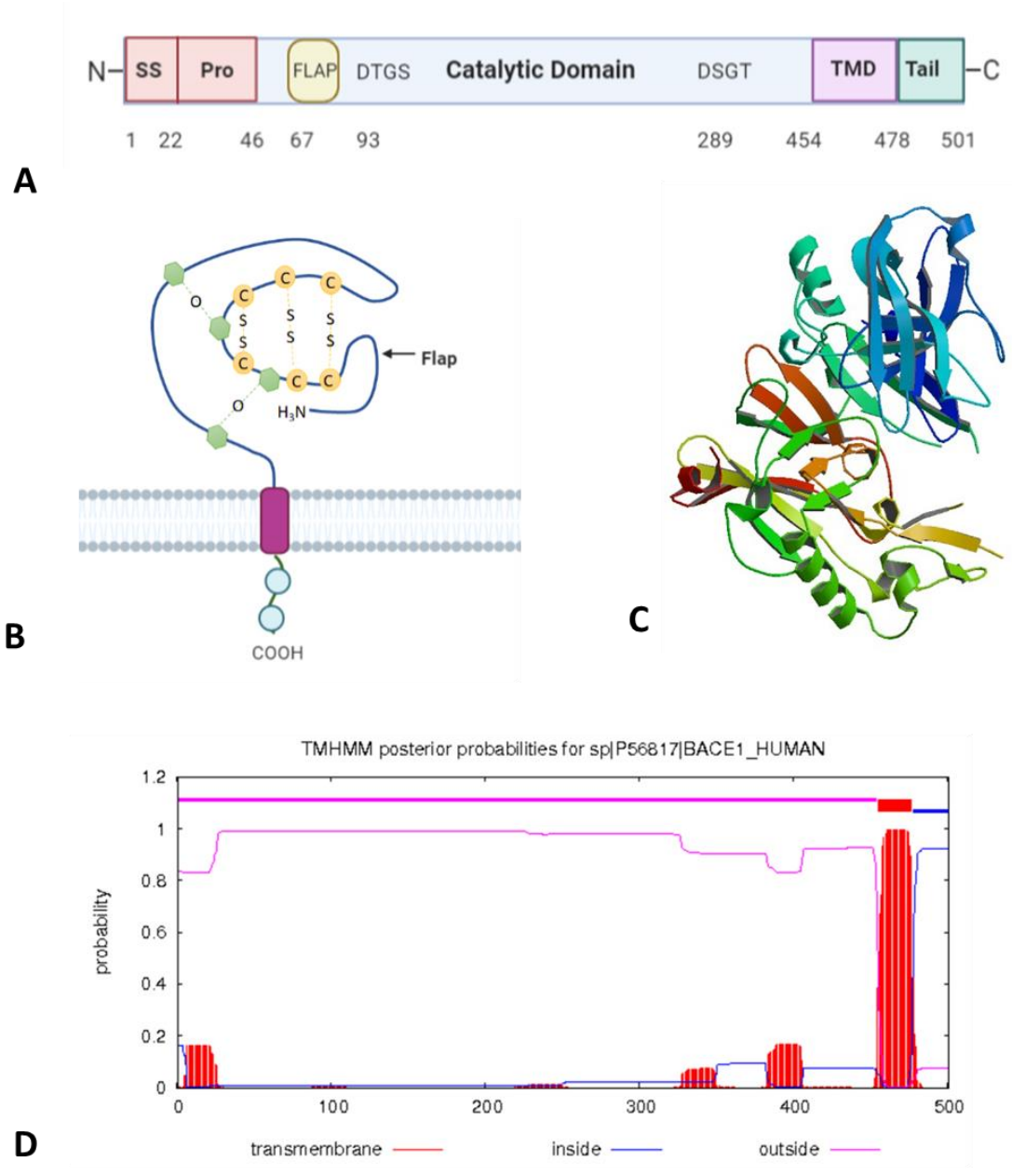

Figure 5: The primary and tertiary structures of BACE1. **A)** A schematic representation of the structures exhibited in BACE1 and their corresponding amino acid residues (adapted from Vassar *et al.*, 2009) **B)** A schematic representation of the mature tertiary structure of BACE1 held together with disulphide bonds

between cysteine residues (yellow circles) and glycosidic bonds between oligosaccharides (green hexagons), with a highly palmitoylated tail (blue circles). **C)** A crystal structure of BACE1 at pH 7.0 (Shimizu *et al*., 2008). **D**) A plot made by TMHMM presenting the probability that certain amino acids span the membrane.

1.4.3 BACE1 in Alzheimer's Disease

Alzheimer's Disease (AD) is a progressive neurodegenerative disorder characterised by memory loss, declining cognitive function, decreased physical function and eventual death (Sathya *et al*., 2012). The pathophysiological hallmark of AD consists of neurotoxic proteins aggregates in the brain, derived from amyloid plaques and neurofibrillary tangles (Sathya *et al*., 2012).

Amyloid plaques are aggregates of hydrophobic Aβ peptides, which are generated by the proteolysis of amyloid precursor protein (APP). Although Aβ production is part of the usual physiology in most cells, at elevated levels it initiates a neurotoxic cascade, leading to neuronal death and dementia.

Like BACE1, APP is a large type-1 membrane protein (770 amino acids), expressed ubiquitously and residing in organelles of the secretory pathway. It is cleaved sequentially to Aβ by β- and γ-secretases in a process known as the amyloidogenic pathway (Figure 6).

BACE1 cleaves the APP ectodomain between methionine (position 671) and aspartic acid (position 672) to generate a secreted APP derivative (sAPPβ) and a membrane-bound C-terminal fragment (β-CTF) of 99 amino acids. The β-CTF is further cleaved by an intramembrane γ-secretase complex, formed by the association of presenilin 1, presenilin 2, anterior pharynx-defective phenotype (APH-1), nicastrin and presenilin-enhancer (PEN-2), to liberate 2 additional products. These include the Aβ peptide which is released into extracellular space and the APP intracellular domain (AICD) which is released into the cytosol. The AICD functions as a transcription factor and also regulates phosphoinositide-mediated calcium signalling (Leissring *et al*., 2002).

The activity of γ-secretases is heterogenous, causing the Aβ peptide to come in varying sizes. In a healthy individual, 90% of Aβ peptides formed are Aβ40. However, the more cytotoxic form, Aβ42, is elevated considerably in AD (Burdick *et al*., 1992; and Vassar *et al*., 2009).

A homolog of BACE1, termed BACE2, shares 64% amino acid sequence similarity. This raised concern regarding its contribution to Aβ peptide production (Vassar *et al*., 2009). However, BACE2 is expressed at low levels in the brain and has a different cleavage site on APP, becoming inferior in the quest for a therapeutic target for preventing AD progression.

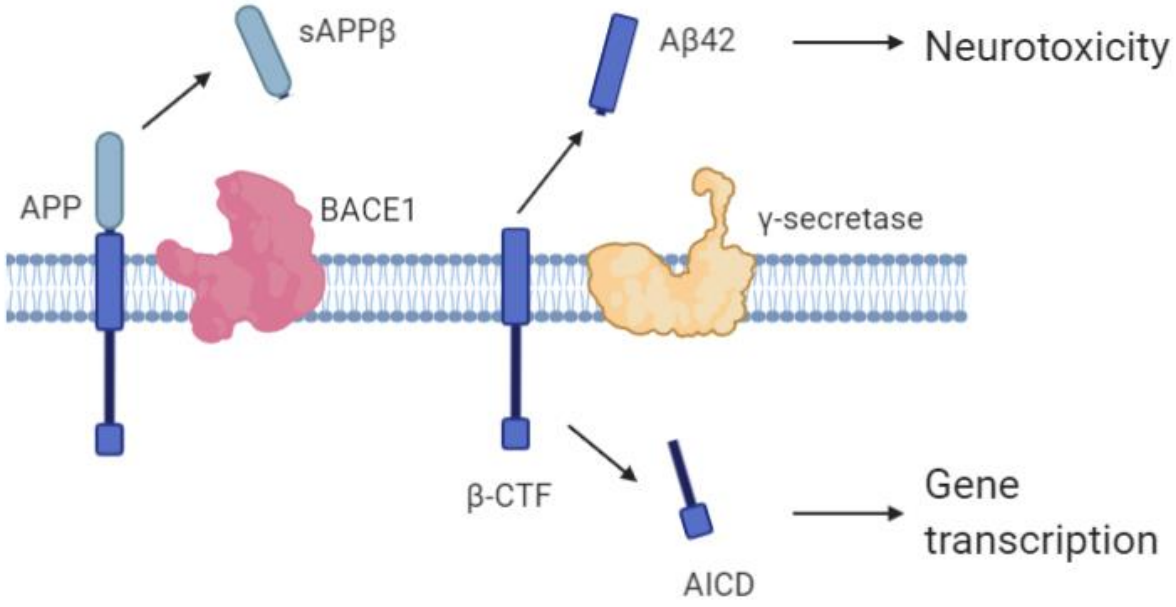

Figure 6: A schematic diagram presenting the amyloidogenic pathway. BACE1 initiates the proteolysis by cleaving APP to sAPPβ and β-CTF. γ-secretases then cleave β-CTF to AICD and Aβ peptides; which are predominately Aβ42 in AD (adapted from Cole & Vassar, 2008*).*

Various α-secretase enzymes, namely ADAM10 and ADAM17, compete with BACE1 for APP. However, they cleave APP at the peptide bond between Lysine (position 687) and Leucine (position 688), generating a sAPPα derivative and a shorter α-CTF with only 83 amino acids (Sathya *et al*., 2012). Again, the γ-secretase complex cleaves the α-CTF, liberating a non-toxic 3Kda peptide (P3).

This alternative sequence of events, most commonly seen in physiology, is known as the non–amyloidogenic pathway and it is thought to antagonize Aβ generation (Stockley & O'Neil, 2008).

The discovery of BACE1 was particularly revolutionary in the field of AD pharmacology, as it is the rate limiting step for Aβ42 production. Extensive efforts focussed on developing compounds to inhibit BACE1 activity in hope of treating AD. Although BACE1 deficient mice are completely absent of Aβ peptides; to date, BACE1 inhibiting drugs have been unsuccessful in preventing cognitive decline in early onset AD in humans (Luo *et al*., 2003). However, the abundance of clinically tested BACE1 inhibitors provides a unique opportunity to rapidly repurpose drugs to treat other BACE1-initiated complications. Hence the focus on BACE1, and not other secretases, in this study.

1.4.4 Other BACE1 substrates

BACE1 has a loose substrate specificity, allowing it to cleave a diverse array of proteins; many of which have been identified using proteomic, bioinformatic and genetic methods (Vassar *et al*., 2014 and Hemming, Elias & Selkoe*,* 2009). This has been invaluable in acquiring knowledge regarding the physiological role of BACE1 and the potential consequences of its absence during pharmacotherapeutic inhibition.

Using proteomics, Hemming *et al* identified a large array of novel BACE1 substrates present in two epithelial cell lines, HEK and HeLa cells (Hemming, Elias & Selkoe*,* 2009). Both cell types were transfected to overexpress BACE1, grown to confluency, then subjected 20 μM GM6001, a metalloprotease inhibitor. GM6001 is thought to enhance BACE1-cleaved products by 2-fold to make their detection easier. From the 116 proteins which were elevated in the over-expressing cells, 68 were soluble products produced from cleaved integral membrane proteins, with 64 being type 1 transmembrane proteins. Therefore, these findings conclude that BACE1 preferentially cleaves type-1 transmembrane proteins.

Many of BACE1's substrates are related to processes of the central nervous system, including: neuregulin 1 (Nrg1) type I and III-β1α, neuregulin 3, seizure protein 6, and sodium gated voltage channel β2 (Navβ2), coinciding with its prime distribution in the brain (Koelsch, 2017). However, BACE1- dependent cleavage of other validated substrates, such as the insulin receptor and Jagged-1/2, could have a potential role in vasculature. Our project will focus on discovering the role of BACE1 in blood vessels, specifically regarding angiogenesis.

1.5.4.1 Insulin receptor

Previously, Turner *et al* investigated the subsite specificity of BACE1 cleavage sites which provides a cleavage sequence profile (Turner *et al*., 2005). This was further exploited by Johnson *et al* in a bioinformatic study which identified 962 potential BACE1 substrates, one of which was the insulin receptor (IR) (Johnson, Chambers & Jayasundera, 2013).

The IR is a tetrameric, membrane bound, tyrosine kinase receptor (TKR), consisting of two extracellular α subunits and two membrane-spanning β subunits (Hubbard, 2013). It can also be present in a truncated soluble form (IRsol) composed of the α-subunits attached to part of the extracellular region of β-subunits. Interestingly, this form is most prevalent in the plasma of individuals with diabetes (Obata *et al*., 2007). Recently, Meakin *et al* discovered the IR is cleaved by BACE1 and that this activity is upregulated in DM (Meakin *et al*., 2018).

BACE1 cleaves the IR in its membrane proximal stalk between Aspartic acid (residue 933) and Lysine (residue 956), releasing the IRsol and a transmembrane fragment consisting of the remaining β-subunits (IR-CTF) (Meakin *et al*., 2018). Like APP, the IR-CTF is further cleaved and degraded by γ-secretase and the proteasome, respectively (Kasuga *et al*., 2007). This proteolytic event leads to insulin resistance in diabetes, suggesting that BACE1 is implicated in the aetiology of diseases other than AD.

1.5.5 BACE1 and diabetes

Various researchers have discovered that BACE1 levels and activity are increased in type 1 and type 2 diabetic models (Devi *et al*., 2012; and Meakin *et al*., 2018). BACE1 expression and activity can be exacerbated under environmental and cellular stresses (Chami & Checler, 2012). These stressors include oxidative stress, inflammation, hypoxia and ischemia; all of which coincide with DM. Although these stressors have primarily been investigated within neuronal tissue within the brain, they could be relevant within an endothelial context.

The BACE1 promoter has multiple binding sites for transcription factors involved in cellular stress including the nuclear factor-κB (NF-κB), the hypoxia-inducible factor 1(HIF-1), Activator Protein 1 (AP-1) and signal transducer and activator of transcription 3 (STAT3) (Chen *et al*., 2012; Zhang *et al*., 2007; Wen *et al*., 2008; Tamagno *et al*., 2008). Therefore, the cellular stress response is involved in upregulating BACE1 expression.

Aforementioned, oxidative stress in an important feature of diabetes. ROS activates the JNK pathway which is involved in regulation inflammation and apoptosis (Mehan *et al*., 2011). Tamagno *et al* showed that H_2O_2 activates the JNK pathway and increases BACE1 expression through its transcription factor, Activator Protein 1 (AP-1). This upregulation was found to be prevented in the presence of JNK inhibitory peptides (Tamagno *et al*., 2008). Notably, BACE1's production of Aβ peptides causes additional oxidative stress and ROS production, producing a vicious positive regulatory loop (Huang *et al*., 1999).

Subsequent investigation by Guglielmotto *et al* discovered two AGEs, pentosidine and glyceraldehyde-derived pyridinium (GLAP), induced BACE1 expression, both *in vivo* and *in vitro* (Guglielmotto *et al*., 2012). Once the AGEs bound their corresponding RAGE receptor, they upregulated BACE1 expression through the consequent activation of NF-κB transcription factor.

Furthermore, in PAD, hypoxia can induce BACE1 expression by ROS production from mitochondria in stressed cells and by activating the HIF-1 transcription factor (Zhang *et al*., 2007).

In conclusion, diabetic-induced insults such as ROS, AGEs and hypoxia stimulate BACE1 expression and activity. Previously, increased BACE1 activity has been found to contribute to the pathogenesis of diabetes through the proteolysis of the insulin receptor, further promoting insulin resistance and subsequent complications (Meakin *et al*., 2018). However, additional investigation is needed to understand whether BACE1 has a specific role in reducing the angiogenic potential of endothelial cells in DM.

1.5.6 BACE1 and VEGFR1 proteolysis

BACE1 deficient mice have been used to analyse the potential effects of BACE1 therapeutic antagonism in AD. Although BACE1 deficient mice were viable, fertile and showed no major morbidity, Cai *et al* discovered that they developed significant retinal pathology (Cai *et al*., 2012). This manifested as retinal thinning, apoptosis and reduced retinal vascular density. These findings may suggest that BACE1 has a role in vascular function.

Following this discovery, the researchers proposed that BACE1 was involved in regulating VEGF signalling. Like APP processing, it was proven that BACE1 acts as a prerequisite to cleave the ectodomain of VEGFR1 (Flt-1), which is subsequently cleaved by γ-secretase to produce a soluble form (sFlt-1) (Cai *et al*., 2012).

Aforementioned, Flt-1 is a negative regulator of VEGF signalling due to it having a 10-fold higher affinity toward VEGF than VEGFR2, but with a 10-fold weaker tyrosine kinase activity (Shibuya, 2011). Although VEGFR2-null mice failed to develop blood vessels and were non-viable, Flt-1-null mice exhibit overgrowth and disorganization of blood vessels. This demonstrates that VEGFR2 is imperative for vascular growth, whereas Flt-1 has a role to negatively regulate it (Shalaby *et al*.,

1995). Moreover, Flt-1 signalling is also important in angiogenesis as it recruits BM progenitor cells to ischemic muscle (Amano *et al*., 2015).

Unlike membrane-bound Flt-1, endogenous sFlt-1 is thought to be completely anti-angiogenic. This activity is produced through two functions; by binding to VEGF and preventing it from signalling through VEGFR2, and by forming non-signalling complexes with membrane bound Flt-1 and VEGFR2 to construct a high affinity negative receptor (Kendall and Thomas., 1993). Thereby, this suggests that BACE1-mediated cleavage of Flt-1 to its subsequent products is anti-angiogenic. Despite the reduced vascular density exhibited in their findings, Cai *et al* suggested that retinal pathology in BACE1-null mice was due to reduced membrane-bound Flt-1 and subsequent negative regulation of VEGFR2. However, our project will focus primarily on how BACE1 activity reduces VEGFR2 signalling.

Interestingly, sFlt-1 levels are increased by 2-fold in diabetics compared to non-diabetics which coincides with increased BACE1 activity and reduced VEGF availability also acquired in individuals with DM (Nandy *et al*., 2010 and Chen *et al*., 2018).

1.5 Overall project aim

This project aims to investigate whether increased BACE1 activity reduces VEGF-mediated angiogenesis in peripheral vasculature of diabetics, contributing to the aetiology of DFUs. Additionally, we aim to determine whether inhibiting BACE1 activity can recover sufficient angiogenic potential to prevent such complications from occurring.

1.6 Hypotheses

1. BACE1 activity reduces pro-angiogenic VEGFR2 signalling.
2. BACE1 inhibitors restore *in vitro* angiogenesis in the context of elevated glucose concentrations.

1.7 Preliminary Data

Unpublished data from the University of Dundee supports our hypothesis that BACE1 inhibition will reverse the anti-angiogenic effects exhibited in models with elevated BACE1 activity. It demonstrates that BACE1 inhibition in HUVECs preserves Flt-1 by 3-fold (Figure 7A-B) and that BACE1-null mice exhibit a dramatic reduction in sFlt-1 levels compared to wild-type mice (Figure 7C). Overall, these results suggest that BACE1 inhibition and deficiency increases Flt-1 and decreases sFlt-1 levels, which is notorious for its anti-angiogenic activity. This project aims to elaborate on these findings and investigate whether BACE1 influences VEGF-mediated angiogenesis.

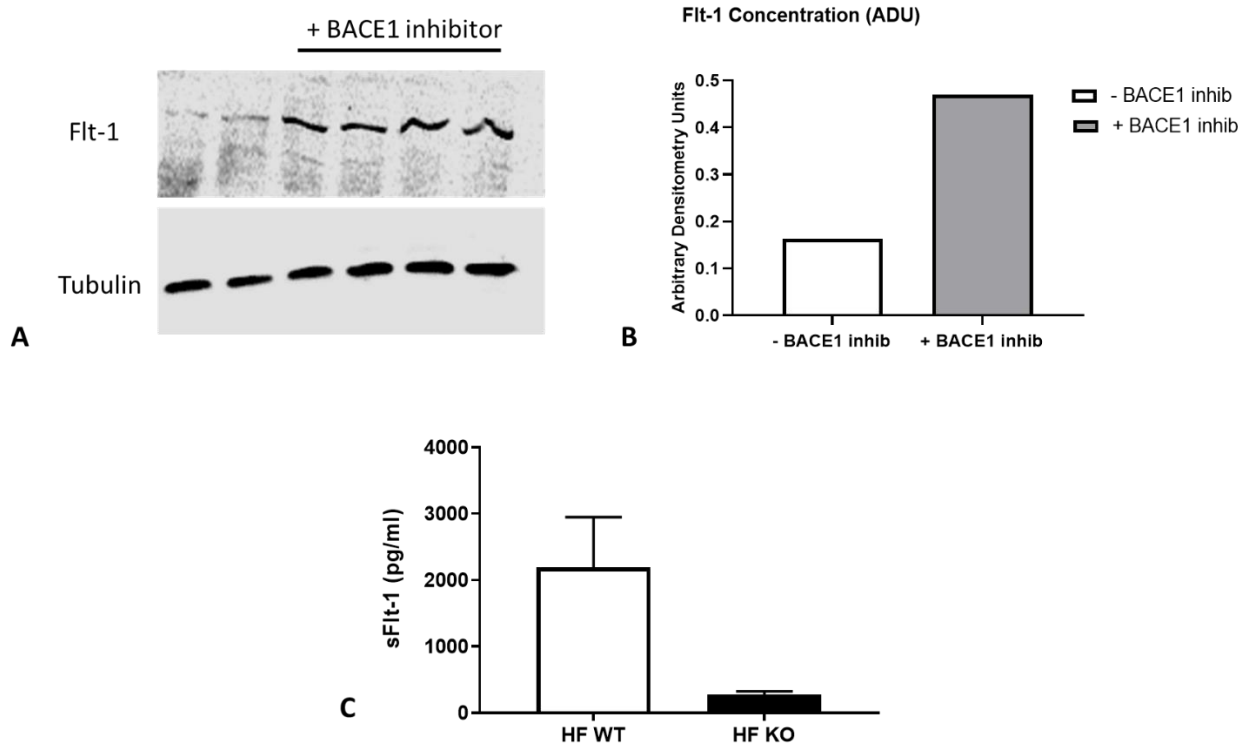

Figure 7: Unpublished data showing that BACE1 inhibition prevents Flt-1 proteolysis. A-B) An immunoblot and graph presenting increased Flt-1 levels in HUVECs treated with a BACE1 inhibitor. **C)** A graph presenting decreased sFlt-1 levels in the plasma of BACE1 KO mice.

2. Materials and Methods:

2.1 Materials

2.1.1 Antibodies and reagents

Table 1: list of primary and secondary antibodies used for Western blotting

Antibody	**Primary or Secondary**	**Species**	**Dilution**	**Company**
Phospho-Enos (Ser1177)	Primary	Rabbit	1:1000	Cell Signalling
Phospho-Akt (Ser473)	Primary	Rabbit	1:2000	Cell Signalling
Akt (total)	Primary	Rabbit	1:1000	Cell Signalling
Enos (total)	Primary	Mouse	1:1000	Cell Signalling
β-actin	Primary	Mouse	1:1000	Santa Cruz
BACE1	Primary	Rabbit	1:1000	Sigma Aldrich
NICD1 (Val1744)	Primary	Rabbit	1:1000	Cell Signalling
GAPDH	Primary	Mouse	1:5000	Fitzgerald
Anti-mouse	Secondary	Goat	1:5000	Sigma Aldrich
Anti-rabbit	Secondary	Goat	1:5000	Sigma Aldrich

Table 2: The reagent used for retinal staining

Antibody	**Primary or Secondary**	**Species**	**Dilution**	**Company**
IsolectinB4-Alexa-488	Primary (conjugated)	Goat	1:100	Invitrogen

2.2 Methods:

2.2.1 Mice

BACE1 $^{-/-}$ mice were obtained from the Jackson Laboratory whereas BACE1 $^{-/+}$ and wild type mice were obtained from a BACE1 $^{-/+}$ X BACE1 $^{-/+}$ breeding strategy. All animal experimentation was performed in accordance with University of Leeds guidelines and regulations of Animals Scientific Procedures Act 1986 (ASPA).

2.2.2 Whole mount immunofluorescent staining of the neonatal mouse retina

2.2.2.1 Tissue collection and immunohistology

On day one of a three-day protocol, the eyes of P5 mice were removed by Dr Paul Meakin after schedule 1 euthanasia and placed in 4% paraformaldehyde for fixation (2 hours, 4^{o}C). The retinas were then dissected by Dr Richard Cubbon according to the Pitulescu *et al*. protocol prior to incubating in blocking buffer (50mL PBS, 0.5% Triton, 0.01% Na deoxycholate, 1% BSA, 0.02% Na Azide, 5µL $CaCl_2$, 5µL $MgCl_2$, 5µL $MnCl_2$, 2% goat serum) (overnight, 4^{o}C) (Pitulescu *et al*., 2010). On day 2, the retinas were rinsed in PBLEC (49.5mL PBS, 0.5mL Triton, 5µL $CaCl_2$, 5µL $MgCl_2$, 5µL $MnCl_2$) for 10 minutes before leaving to incubate in in IsolectinB4-Alexa-488 (table 2) dissolved in PBLEC (overnight, 4^{o}C). On the final day, the retinas were washed 3 X 20 minutes (room temperature) in PBS and 0.2% Triton before being mounted on slides using Prolong Gold.

Images were taken by Dr Richard Cubbon using a LSM880 upright Confocal Microscope (Zeiss) with both 10X and 40X objectives.

2.2.2.2 Image analysis

Images were analysed with FIJI (ImageJ). Each whole mount image (10 X objective) was analysed for the following parameters (Figure 8); (1) radial outgrowth (µm): the length from the centre of the

retina to the perimeter. (2) Area of vasculature (µm^2): the ratio of threshold vascular endothelial pixels that have been selected in the region of interest (ROI) to the total number of pixels in the ROI. (3) Branching complexity: the number of branch points observed in a H:200 X W:200-microns ROI using the cell counter plugin tool.

Different parameters were analysed in 40X objective images collected at the emerging angiogenic front (Figure 8); (1) Average tip cells per mm of vascular front (µm): the vasculature at the parameter was measured and the number of tip cells along this were counted to give an indication of tip cell quantity. (2) Average number of filopodia per tip cells: total filopodia were counted from tip cells using the cell counter plugin tool and divided by the number of tip cells.

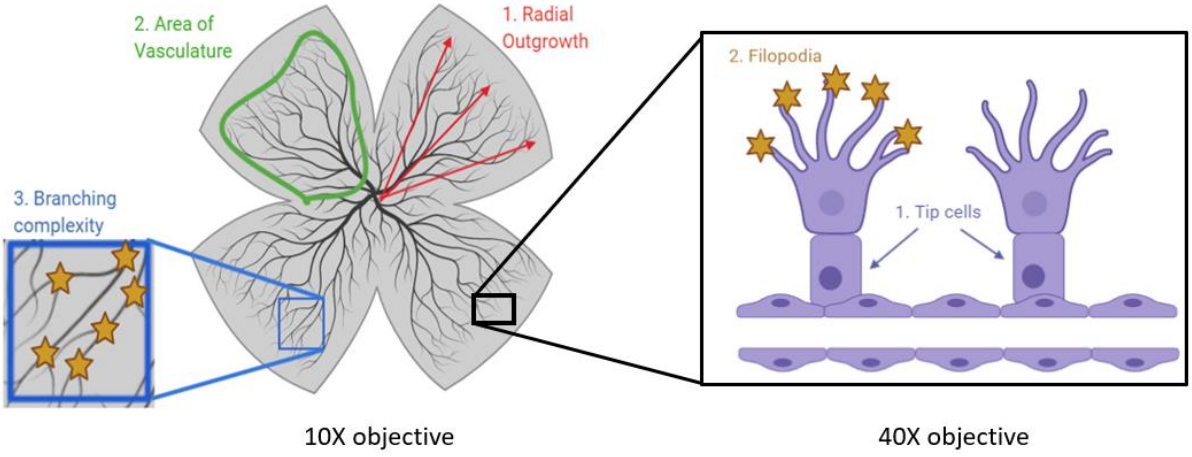

Figure 8: A diagram showing the parameters measured in both the 40X and 10X objective images of the retina (adapted from Rust *et al.*, 2019). The radial outgrowth, area of vasculature and branching complexity were measured using the 10X objective images, whereas the number of tip cells and filopodia were measured using the 40X objective images.

2.2.2.3 Statistical analysis

GraphPad Prism 8.0 software was used to observe vasculature differences in genotypes using graphs. Unfortunately, due to the Covid-19 lockdown, statistical significance could not be analysed because of the limited number of repeats acquired.

2.2.3 Primary cell Isolations and culture

2.2.3.1 Human Saphenous Vein Endothelial Cells (HSVECs)

Saphenous veins were removed during surgery at Leeds General Infirmary. The vein was placed on a sylgard-coated petri dish and carefully opened along its longitudinal axis with a scalpel blade. HSVECs were obtained by pinning the vein luminal face open and incubating it in 1mg/mL collagenase- Type 2 (Worthingtons) (10 minutes, 37^{o}C). The vessel was washed several times with endothelial wash solution (DMEM, 4.5% Fetal Bovine Serum, 2mM L-glutamine and 1 X Penicillin-Streptomycin) and the collagenase/wash solution mix was collected and centrifuged (6 minutes, 600g, 4^{o}C). Subsequently, the pellet was resuspended in wash solution and centrifuged a second time (10 minutes, 600g, 4^{o}C). Lastly, the pellet was resuspended in Endothelial Cell Growth Medium MV2 (PromoCell) and each vein was plated into 1 well of a 6-well plate. Media was changed every 2-3 days until cells were confluent.

2.2.3.2 Pulmonary Endothelial Cells (PECs)

Lungs were harvested by Dr Paul Meakin from either WT or BACE1 $^{-/-}$ mice and homogenised in 1mg/mL collagenase-Type 2 (Worthingtons) prior to being incubated whilst rotating (45 minutes, 37^{o}C). The homogenate was then passed through 70µM cell strainer and centrifuged in a benchtop 5810R (5 minutes, 1200rpm, 5^{o}C). The pellet was washed in 1% BSA/PBS mix and centrifuged further (5 minutes, 1200rpm, 5^{o}C). The subsequent pellet was incubated whilst rotating with a CD146 mouse microbead (20 minutes, 4^{o}) before being spun (5 minutes, 4000rpm) and passed through a magnetic column with the aid of 1% BSA/PBS mix. Remaining cells were released from the column and spun a final time (5 minutes, 400rcf) before being resuspended in Endothelial Cell Growth Medium MV2 (PromoCell) and seeded into 6-well plates/ T75 flasks accordingly. The media was changed 2 hours later, 24 hours later and alternate days until the cells reached confluency.

2.2.3.3 Human Umbilical Vein Endothelial Cells (HUVECs)

HUVECs (PromoCell) were seeded at 7.5 X 10^5 in a T75 flask with Endothelial Cell Culture Medium 2 (ECGM-2) (PromoCell) and incubated (37 °C). Once confluent, cells were harvested by incubating with trypsin-EDTA 0.25% (3 minutes, 37°C). They were then collected by centrifugation (5 minutes, 500rcf) prior to being resuspended in ECGM-2. HUVECs at passage 4 were used for the fibrin gel angiogenesis assays and passage 5 for the VEGF stimulation assays.

2.2.4 Fibrin gel angiogenesis assay

2.2.4.1. HUVECs

The fibrin gel angiogenesis assay was adapted from Nakatsu *et al* (Nakatsu *et al*., 2007). Briefly, HUVECs were incubated with Cytodex-3 beads (Amersham) at a concentration of 400 cells/ bead (4 hours, 37°C) before being transferred into a T-25 flask and incubated overnight (37°C). The HUVEC-coated beads were resuspended in a of 2 mg/mL fibrinogen-Type-1 (Sigma-Aldrich) solution containing 0.15 U/mL aprotinin (Sigma-Aldrich), 5 ng/mL FGF-2, and 5 ng/mL VEGF. Where indicated, BACE1 inhibition was achieved by adding 250nM β-Secretase Inhibitor IV (M3) to the fibrinogen solution and 250nM DMSO was used as a relevant control. 500µL of fibrinogen-bead suspension was mixed with 12.5µL thrombin (Sigma-Aldrich; 50 U/ml) in each well of a 24-well plate and left to clot (5-10 minutes, room temperature). After a short incubation (15 min, 37°C), 1mL of ECGM-2 was added dropwise to cover each clot before leaving the plate to incubate (24 hours, 37°C). Sprout formation was imaged at a 10X magnification with an Olympus Microscope equipped with a camera. The sprouts of 40 beads/condition (10 beads from each well) were analysed using Image-J software.

2.2.4.3 Statistical analysis

GraphPad Prism 8.0 software was used to analyse differences in sprouting in each genotype by using a T-test. The standard error of the mean (SEM) was represented by error bars on each graph and the differences were considered significant at *P<0.05, **P<0.01 and ***p < 0.001.

2.2.5 VEGF stimulations

2.2.5.1 HUVECs

200,000 HUVECs were seeded into each well of a 6-well plate and cultured until confluent. Once confluent, cells were serum starved in ECGM-2 (absent of growth supplements but added 0.1% Foetal Calf Serum). Here, 1ml of serum starved ECGM-2 media containing either 250nM M3 or DMSO was added to each well prior to incubating (24 hours, 37°C).

The following day, 2ug/ml or 20ug/ml VEGF was added to its allocated well (Figure 9) before being incubated (30 minutes, 37°C). After the VEGF stimulation, the cells were incubated with 100µL of Cell Extraction Buffer supplemented with 1µL of both phosphatase and protease inhibitors (4 minutes, -20°C). The lysed cells were collected into an Eppendorf using a tissue scraper and immediately frozen at -20°C.

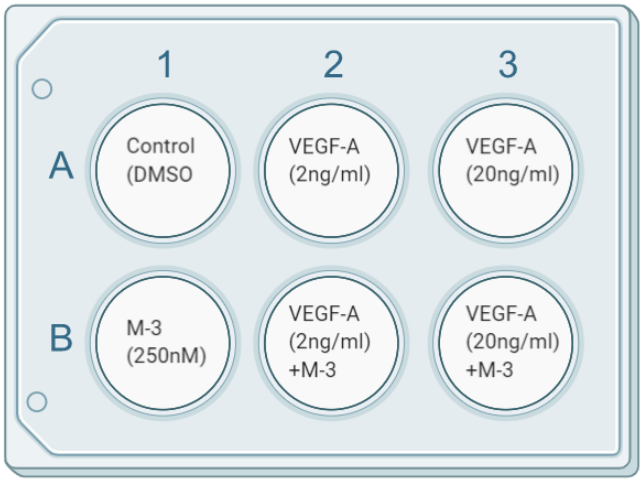

Figure 9: The specific conditions each well was exposed to, including relevant controls.

2.2.5.2 Pulmonary Endothelial Cells

Once PECs had been isolated and seeded, as described in 2.2.3.2, they were cultured until confluency. The cells were then serum starved in MV2 (absent of growth supplements but added 0.1% Foetal Calf Serum) (24 hours, 37^{o}C) prior to being stimulated, lysed and harvested identically to the HUVECs mentioned above (2.2.5.1).

2.2.6 BCA protein quantification

Protein quantification was done according to manufacturer's instructions using Pierce™ BCA Protein Assay Kit (Sigma Aldrich). HUVEC and PEC protein lysate samples, from previous VEGF stimulation assays, were defrosted on ice, centrifuged (15 minutes, 14,000rcf, 4^{o}C) before the pellet was discarded. The supernatant of each sample was diluted 1:8 in dH_2O and 25µl of the diluent was added to duplicate wells of a 96-well plate. Fresh BCA reagent was prepared and 200µL was added to each well, mixed by shaking, and incubated (30 min, 37 °C). The absorbance at 562 nm was measured immediately with a Microplate Spectrophotometer (Bio-Tek Powerwave). The protein's absorbance was normalised by protein standards which fitted a linear equation, this enabled the protein concentration to be obtained.

2.2.7 Western blotting

2.2.7.1 SDS-PAGE electrophoresis

Samples were made to their required concentration with NuPAGE™ 10X reducing agent and 4X sample buffer (Invitrogen). 7µL of pre-stained ladder (BioRad) and 20µL of samples were loaded into 4-12% Bis Tris NuPAGE™ gels (Thermo Fisher). The gel was submerged in 1X NuPAGE™ MES running buffer and separated by electrophoresis (110V, 2 hours).

2.2.7.2 Trans-blot Turbo Transfer System (BioRad) Western blotting for NICD1

Following SDS-PAGE, proteins were transferred onto a nitrocellulose membrane using a trans-blot Turbo Transfer System (BioRad) assembled according the manufacturer's instructions. Transfer buffer (BioRad) (1 X buffer: 1X ethanol: 3 X dH_2O) was used to wet 2 X pre-made filter-paper stacks and a nitrocellulose membrane which was used to assemble a 'blotting sandwich' encasing the gel. The sandwich was assembled on the dry transfer system and the proteins were transferred by electrophoresis (high MW, 10 minutes).

The membrane was incubated (1 hour, room temperature) in 5% milk in TBST (TBS/0.02% Tween-20) before being incubated in the NICD1 primary antibody (table 1) (overnight, 4^{o}C). The following day, the membrane was washed with 3 X 10 minutes washes in wash buffer (TBS/0.02% Tween-20) before being blocked again in 5% milk in TBST (1 hour, room temperature). Following the second block, the membrane was incubated in the secondary anti-rabbit antibody (table 1) diluted in blocking reagent (5% BSA in 0.1% TBS/Tween-20, pH7.4) (1 hour, room temperature). The membrane was further washed 3 X 10 minutes with wash buffer before being developed with ECL immobilon substrates (Sigma Aldrich) according to manufacturer's instructions.

The membrane was then washed 3 X 10 minutes with wash buffer prior to being incubated in the GAPDH primary antibody (table 1) (45 minutes, room temperature). Further 3 X 10 minutes washes were made before incubating in the secondary antibody (table 1) (45 minutes, room temperature). A final 3 X 10 minutes washes were made of the membrane before it was developed with ECL immobilon substrates (Sigma Aldrich), according to manufacturer's instructions, and imaged using GeneSys imager software. Lastly, the image was analysed using ImageJ software.

2.2.7.3 Wet transfer Western blotting for all other antibodies

Following SDS-PAGE, proteins were transferred onto a PVDF membrane (Thermo Fisher). A wet transfer cassette was assembled whilst soaked in transfer buffer (6.06g Tris Base, 28.84g glycine, 400ml methanol made up to 2L with dH_2O). The cassette included the SDS-PAGE gel and a PVDF membrane sandwiched between two transfer sponges and two filter papers. The cassette was placed in a transfer tank and submerged in transfer buffer. Proteins were transferred by electrophoresis at 100V for 1 hour. The membrane was then incubated (30 minutes, 37^{o}C) in blocking reagent (5% BSA in 0.1% TBS/Tween-20, pH7.4) before being incubated with the primary antibody diluted to the correct concentration (table 1) in blocking reagent (overnight, 4^{o}C).

The membrane was then rinsed 3 X 10 minutes in wash buffer (TBS/0.02% Tween-20) before being incubated with the correct concentration of complimentary secondary antibody (table 1) diluted in wash buffer (1 hour, room temperature). Next, the membrane was washed 3 X 10 minutes with wash buffer before being developed with ECL immobilon substrates (Sigma Aldrich) according to manufacturer's instructions. Finally, the membrane was imaged using GeneSys imager software and analysed using ImageJ.

2.2.7.4 Statistical analysis

GraphPad Prism 8.0 software was used to analyse differences in signalling protein abundance in different groups by using T-tests and two-way analysis of variance (ANOVA) coupled with Sidak post-hoc test. The standard error of the mean (SEM) was represented by error bars on each graph and the differences were considered significant at *P <0.05.

3. Results

3.1 BACE1 deficiency alters developmental angiogenesis

To observe the effects of BACE1 in developmental angiogenesis, confocal microscopy was performed on retinas from P5 wild-type (WT, N=2), BACE1 heterozygous (Het, N=3) and BACE1 knock-out (KO, N=1) mice. Retinas were dissected and stained with IsolectinB4-Alexa-488 which fluorescently highlighted endothelial cells in green. Images of the whole mount retina were taken with a 10X objective, whereas sprouting tip cells and filipodia were visualised with a 40X objective. The resulting images were analysed using FIJI (Image J) software.

Whole mount retinas were used to analyse various parameters including radial outgrowth, branching complexity and vascular area. Results showed that the KO mouse had a nominal reduction in radial outgrowth (µm) compared to WT and Het mice (WT= 1540 µm, Het= 1506 µm and KO= 1291 µm) (Figures 10A-D). Additionally, the KO mouse had increased number of branch points within its vasculature compared to the other genotypes (WT= 1081.5 ± 169.9 mm^2, Het= 1050 ± 33.03 mm^2 and KO= 1257.75 mm^2) (Figures 10E-H). Lastly, the vascular area was increased in the KO mouse compared to WT and Het mice (WT= 37.88 ± 3.293 %, Het= 39.13 ± 1.576 % and KO= 41.51 %) (Figure 10N).

Images of the developing vascular front revealed that the KO mouse tended to have fewer tip cells per mm of vascular front compared to the other genotypes (WT= 22.03, Het= 26.34 and KO= 18.18) (Figure 10M). In contrast, the KO mice were inclined to have more filopodia per tip cell compared to the other genotypes (WT= 12.26, Het= 13.50 and KO= 13.81) (Figures 10 I-L).

Due to the Covid-19 pandemic, repeats of this experiment could not be completed to assess the reliability and statistical significance of these findings. However, these results present a potential role of BACE1 in developmental angiogenesis, which merits further investigation.

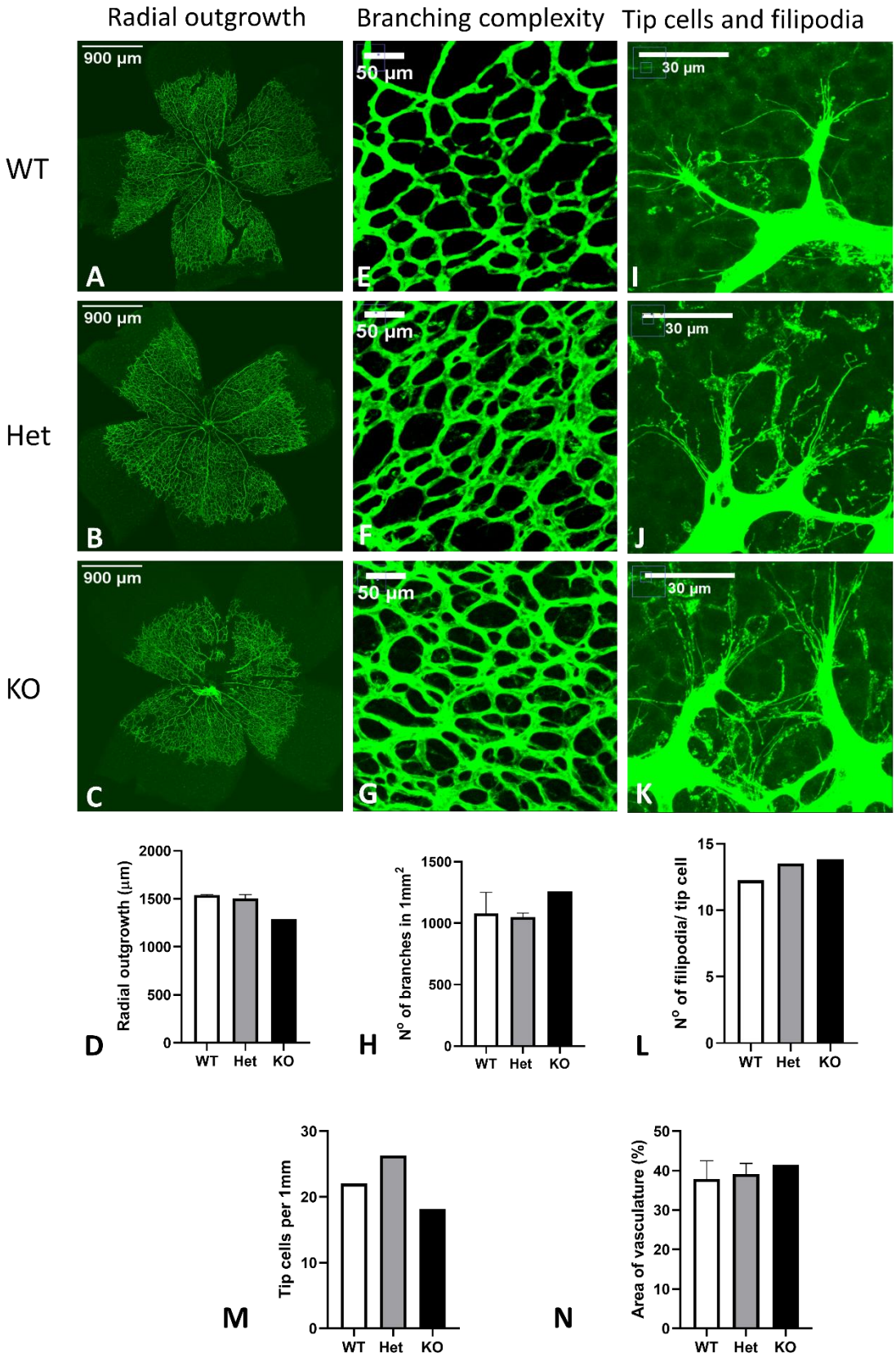

Figure 10: BACE1 deficiency causes aberrant developmental angiogenesis. A-C) Confocal microscopy images of whole mount retinas from WT (N=2), Het (N=3) and KO (N=1) mice taken with a 10X objective, scale bar 900µm.

D) Mean radial outgrowth for each genotype (µm). **E-G)** Confocal microscopy images of retinas from WT, Het and KO mice taken with a 10X objective to show branch points, scale bar 50µm. **H)** Mean number of branch points in $1mm^2$ for each genotype. **I-K)** Confocal microscopy images of tip cells and their protruding filipodia from WT, Het and KO mice taken with a 40X objective lens, scale bar 30µm. **L)** Mean number of filopodia per tip cell for each genotype. **M)** Mean number of tip cells per 1mm of vascular front for each genotype **N)** Mean percentage area of vasculature for each genotype. Data are means ± SEM.

To further study the role of BACE1 in angiogenesis, additional experiments were completed *in vitro*. This allowed stringent manipulation of variables within various assays so that physiological differences and signalling factors of angiogenesis could be analysed.

3.2 HUVECs are a suitable cell-type for investigating the role of BACE1 *in vitro*

To investigate which endothelial cell type would be a suitable model for studying the role of BACE1 *in vitro*, an immunoblot was completed using mouse primary pulmonary endothelial cells (PECs, N=1), human umbilical vein endothelial cell (HUVECs, N=1) and human primary saphenous vein endothelial cells (SVECs, N=1). All cell types were grown to confluency, lysed to release protein content then immunoblotted for BACE1 using an anti-BACE1 antibody specific to its N-terminus residues (46-62). Densitometry values were normalised to the expression of the house keeping protein, β-Actin, to give the arbitrary densitometry units (ADU) for each cell-type. Here, values displayed that HUVECs had abundant levels of BACE1 compared to other cell types (WT PEC= 0.10 ADU, KO PEC= 0.00 ADU, HUVECs=0.82 ADU and SVECs= 0.04 ADU) (Figures 11A-B). This suggests that substantial manipulation of BACE1 activity in HUVECs can be achieved using BACE1 inhibitors, providing an ideal setting for studying its role in angiogenesis and the therapeutic potential of BACE1 inhibitors.

Additionally, the immunoblot revealed that PECs were also suitable for this investigation. WT PECs had detectable quantities of BACE1, whereas KO PECs were completely deficient, confirming their genotype and the specificity of the antibody. Comparing the differences in the *in vitro* phenotype of WT and KO PECs will provide invaluable information regarding the role of BACE1 in angiogenesis. Lastly, primary isolated SVECs show low levels of BACE1 protein, indicating that other cell types are more suitable experimental models.

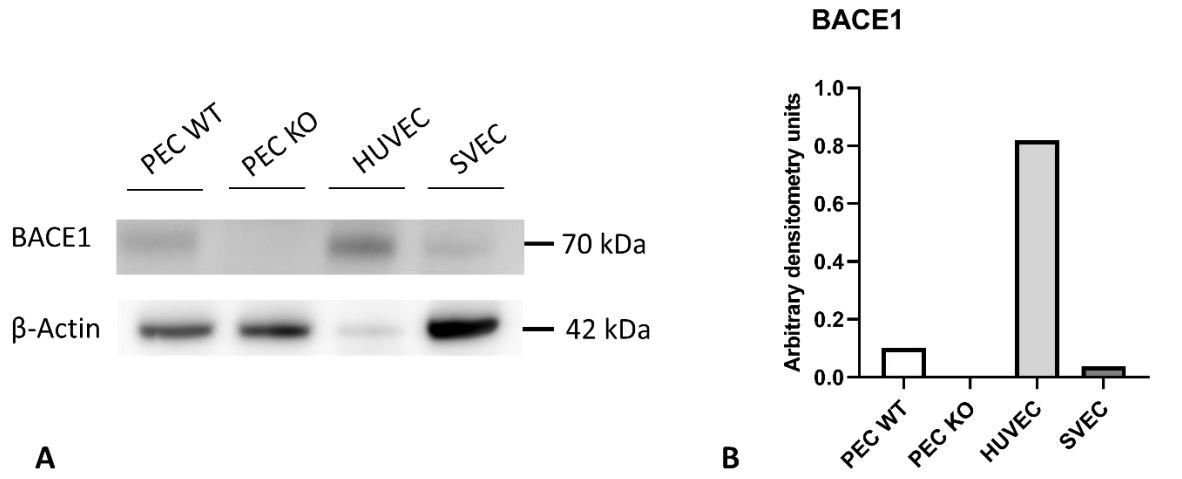

Figure 11: HUVECs abundantly express BACE1. A-B) PECs, HUVECs and SVECs (N=1) were grown to confluency, lysed and analysed by an immunoblot for BACE1. Densitometry values produced for each cell type were normalised to the house keeping protein, β-Actin, to produce arbitrary densitometry units (ADU).

Once suitable endothelial cell types were identified, further *in vitro* examination regarding BACE1's role in angiogenesis was achieved.

3.3 BACE1 inhibition increases angiogenic sprouting in HUVECs

To explore the role of BACE1 in angiogenesis, an *in vitro* fibrin gel angiogenesis assay was completed. HUVECs were coated onto Cytodex-3 beads and embedded in a fibrin-mesh containing essential growth factors such as VEGF. Subsequently, the cells were treated for 24 hours with 250nM β-

Secretase Inhibitor IV (M3), a potent and highly specific BACE1 inhibitor, or its appropriate vehicle control, dimethyl sulfoxide (DMSO). Following the incubation, light microscopy images were taken and the number and length of sprouts of each bead was analysed using ImageJ.

Two concentrations of M3, 250nM and 1µM, were used in early experiments to investigate the optimal concentration for the assay. These concentrations were chosen based on the IC50 values of M3's substrates and their use in previous investigations (Sigma-Aldrich, 2020 and Hamilton *et al*., 2014). Results revealed that 250nM M3 produced a statistically significant increase in the number of sprouts compared to the DMSO control, whereas 1µM M3 concentration did not (DMSO= 10.02 ± 0.5424, 250nM M3= 11.62 ± 0.4618, 1µM M3= 10.51 ± 1.329, P=0.05) (Figure 12A-C). This remained statistically significant when expressed as a relative percentage increase versus control (17.07 ± 3.354, P=<0.001) (Figure 12E). Therefore, 250nM M3 was used in subsequent experiments. Moreover, as M3-treatment did not affect sprout length (DMSO=108.3 ± 7.290 µm ±, 250nM M3 = 110.2 ± 6.600 µm, 1µM M3 = 99.6 ± 14.77 µm), this result could suggest that M3 promotes tip cell selection which, unlike stalk cells, are not characteristic of cellular proliferation (Figures 12C-F).

To investigate whether 250nM M3 might be promising as a therapy to improve the angiogenic potential of individuals with DM, the embedded HUVECs were incubated for 24 hours in either 5mM or 30mM glucose to mimic an exaggerated hyperglycaemic state. HUVECs incubated in 30mM glucose and treated with 250nM M3 did not show a statistically significant increase in sprout number (DMSO= 10.10 ± 0.7149, 250nM M3= 10.42 ± 0.2260 , P= ns) or a statistically significant percentage increase versus control (5.945% ± 5.335, P=ns), indicating that high glucose concentrations eliminate the effects of M3 (Figures 12C-F). However, when analysing the average sprouting area (μm^2) of each bead by multiplying the average number of beads by the average length of sprouts, both the 5mM (DMSO= 750.8 ± 50.52μm^2 and 250nM M3= 1020 ± 61.12 μm^2, P=<0.01) and 30mM (DMSO= 812.5 ± 37.77 μm^2 and 250nM M3=1105 ± 53.14 μm^2, P=<0.01) glucose

concentrations were found to have a significant increase in sprouting area when treated with 250nM M3 (Figure 12G).

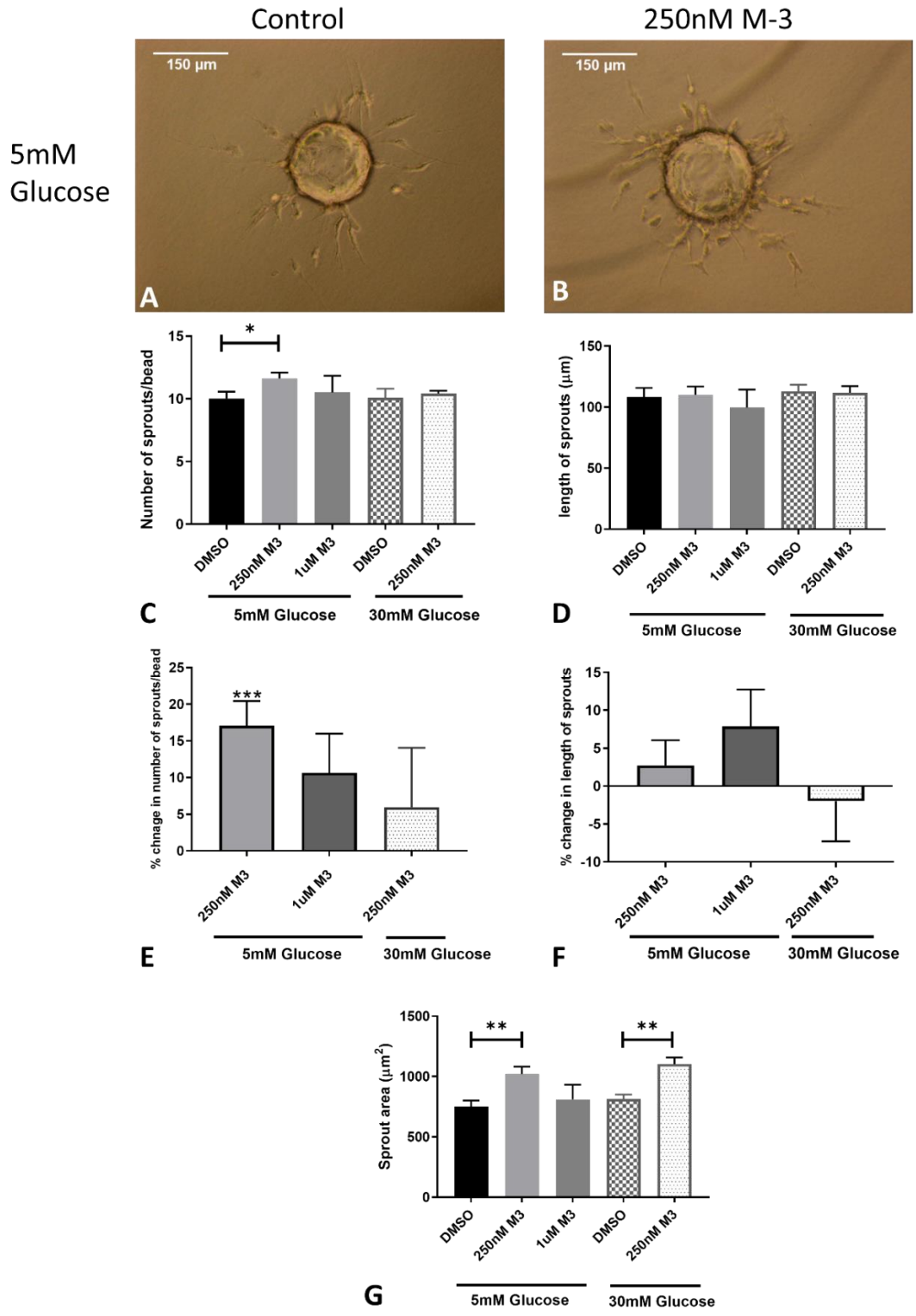

Figure 12: M3 increases angiogenic potential in HUVECs. A-B) Light microscopy images of sprouted beads, treated with 250nM M3 or DMSO, taken with a 10x objective, scale bar 150µm. **C)** Mean number of sprouts

per bead for HUVECs incubated in 5mM glucose treated with DMSO (N=9), 250nM M3 (N=9) or 1µM (N=3) and 30mM glucose treated with DMSO (N=6) or 250nM M3 (N=6). **D)** Mean length of sprout (µm) per bead for each condition. **E)** Percentage change in number of sprouts per bead for each condition. **F)** Percentage change in length of sprouts for each condition. **G)** Mean sprout area (μm^2) for each condition. Data are means ± SEM. Statistical analyses were made using unpaired T-tests. *p < 0.05; ** p<0.01; ***p < 0.001.

These results demonstrate that 250nM M3 can significantly increase angiogenic sprouting in normal glucose concentrations. Therefore, further investigation was completed to uncover the mechanism of M3-induced angiogenic sprouting.

3.4 BACE1 inhibition increases VEGF induced sprout formation

To study how M3 promotes sprout formation in HUVECs, the *in vitro* fibrin gel angiogenesis assay was performed by adding varying concentrations of VEGF to the fibrin clot: 0ng/mL, 0.5ng/mL and 5.5ng/mL. The ECGM-2 media which supports angiogenesis in the fibrin clot contains foetal calf serum (FCS); which provides a basal level of VEGF, emphasizing that the stated VEGF concentrations are additional. Results showed a positive correlation between VEGF concentrations and the additional number of sprouts formed in the presence of M3 (Figures 13A-B).

When HUVECs were treated with 250nM M3, those which had been incubated with supplementary 5.5ng/mL VEGF had a statistically significant increase in sprout formation (DMSO= 10.02 ± 0.5424 and 250nM M3= 11.62 ± 0.4618, P=<0.05), whereas those incubated in 0.5ng/mL VEGF (DMSO= 8.395 ± 0.8649 and 250nM M3= 8.987 ± 0.9816) and 0.0ng/mL (DMSO= 11.07 ± 0.3576 and 250nM M3= 10.73 ± 0.3941) did not (Figures 13A). Additionally, when observing the percentage increase in sprout numbers, HUVECs treated with 250nM M3 and incubated in an extra 5.5ng/mL VEGF had a statistically significant increase (17.07 ± 3.354, P=<0.001) unlike those incubated in extra 0.5ng/mL VEGF (6.817 ± 2.685, P=ns) and 0.0ng/mL (-3.078 ± 0.4288, P=ns) (Figures 13B). The negligible effects

on sprout length in all three VEGF concentrations support previous findings that M3 specifically effects sprout formation (Figures 13C-D).

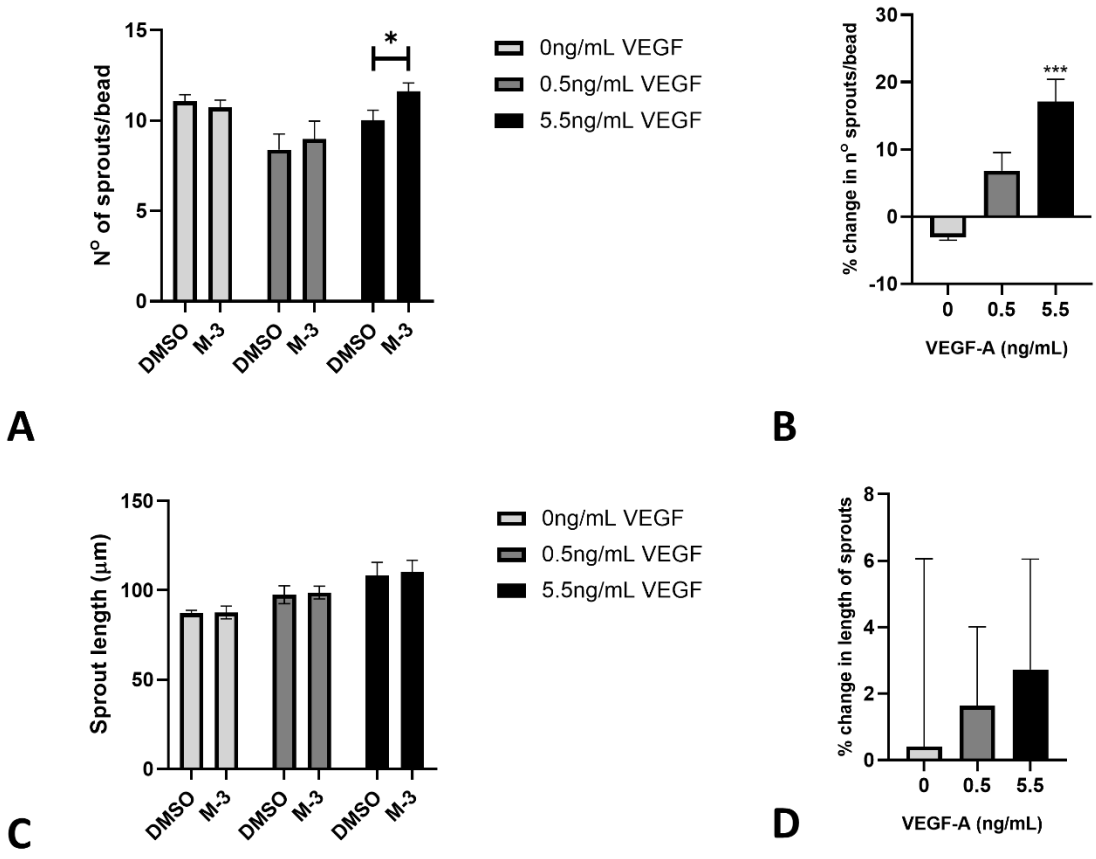

Figure 13: M3 encourages sprout formation through VEGF signalling. A) Mean number of sprouts per bead for each condition: 0ng/mL (N=2), 0.5ng/mL (N=5) and 5.5ng/mL (N=9) **B)** Percentage difference in number of sprouts per bead induced by M3 for each condition. **C)** Mean sprout length (µm) for each condition**. D)** Percentage difference in length of sprouts for each condition. Data are means ± SEM. Statistical analyses were made using unpaired T-tests. *$p < 0.05$; ***$p < 0.001$.

In conclusion, these results suggest that M3 potentiates the pro-sprouting effect of VEGF. Therefore, further inquiry into the effects of BACE1 inhibition on VEGF signalling was conducted.

3.5 BACE1 inhibition has nominal effects on signalling factors downstream of VEGFR2

To further explore the impact of M3 on VEGF signalling, phosphorylation events downstream of VEGF binding to VEGFR2- at eNOS (Ser1177) and Akt (Ser473)- were analysed. Two suitable endothelial cell types, HUVECs and PECs, were grown to confluency before being serum starved for 24 hours and stimulated with either 0ng/mL, 2ng/mL or 20ng/mL VEGF for 30 minutes. Following the stimulations, the cells were lysed and immunoblots were performed for phosphorylated and total protein. The densitometry values were normalised to β-Actin and the ADU was retrieved for each condition.

In HUVECs, immunoblot analysis of protein lysates revealed that phosphorylation events for both eNOS and Akt increased in cells treated with 250nM M3. This was particularly noticeable for phosphorylated eNOS (p-eNOS) in cells which had not been stimulated (0ng/mL VEGF) (p-eNOS = 0.8251 ± 0.2165 increase, P=0.05), suggesting that M3 significantly increases basal levels of p-eNOS. This is also true for basal phosphorylated Akt (p-Akt), but to a much lesser extent (p-Akt= 0.1755 ± 0.2862 increase) (Figures 14A-D).

Expectedly, increased VEGF concentrations caused p-eNOS (Ser1177) levels to rise in both conditions (Figure 14A, C). This suggests that a 30-minute VEGF stimulation is an optimal timeframe in HUVECs for measuring p-eNOS. Furthermore, the significant increase of p-eNOS shown at 0ng/mL VEGF did not persist when VEGF concentrations increased. This may suggest that p-eNOS is saturated; therefore, M3 cannot have any further effect (Figure 14C). Again, this finding was less obvious with p-Akt; however, overall p-Akt increased, particularly with a 20ng/ mL VEGF (control= 0.6397 ± 0.6897 increase, 250nM M3= 0.4643 ± 0.6966 increase) (Figure 14D).

Interestingly, total eNOS and Akt protein levels increased with BACE1 inhibition (Figure 14E-F). Although total protein levels are not indicative of activity, this finding shows that BACE1 inhibition may influence protein expression. Moreover, the ratio of phosphorylated protein to total protein

was calculated for both eNOS and Akt to analyse their activity in relation to their expression (Figure 14G-H). Results displayed a slight positive correlation between VEGF concentrations and eNOS activity in both the control and treated HUVECs (Figure 14G). Contrastingly, this correlation was absent when observing the p-Akt to total Akt ratio (Figure 14H).

In PECs the basal levels of p-eNOS was also increased in cells treated with 250nM M3 (0.2226 ± 0.02463 increase), although phosphorylation of Akt was not (-0.3847 ± 0.04177 decrease) (Figure 14I-L). Unlike HUVECs, there was no positive correlation between phosphorylation events and VEGF concentrations in WT PECs, possibly suggesting that the timeframe for peak phosphorylation events in PECs differs from HUVECs (Figure 14K-L). Therefore, future experiments assessing VEGF stimulation in PECs may require a shorter timeframe so that peak phosphorylation events can be analysed. BACE1 KO PECs presented similar p-eNOS levels to untreated WT PECs.

Lastly, the ratio of p-eNOS to total eNOS presents an increase in eNOS activation in PECs treated with 250nM M3, particularly at 0ng/ mL concentration (0.3601 ± 0.1161 increase) (Figure 14O). This increase is obtained throughout VEGF stimulations, suggesting that M3 causes increased eNOS activation in PECs. Like HUVECs, this effect is absent in p-Akt as both KO and M3 treated PECs have reduced Akt activation (Figure 14P).

The differences between chronic and acute BACE1 inhibition could be observed in KO and M3 treated PECs, respectively. Firstly, chronic BACE1 inhibition showed almost a 2-fold increase in total eNOS protein (0.9336 ± 0.4548 increase). This suggests that BACE1 inhibition causes an increase in eNOS protein expression, which in turn reduces the relative proportion of p-eNOS to total eNOS (Figure 14M). Contrastingly, acute BACE1 inhibition had no effect on eNOS expression, demonstrating an increase in proportion of phospho-proteins and subsequent eNOS activity. Total Akt protein was also increased in response to chronic BACE1 exposure, but to a lesser extent (0.3686 ± 0.1212 increase).

A decrease in total eNOS levels was observed once BACE1 KO PECs were stimulated with increasing concentrations of VEGF. Whereas M3 treated cells followed a similar pattern of eNOS expression to WT cells, suggesting that unlike chronic BACE1 inhibition, acute BACE1 inhibition does not affect eNOS protein expression. Total Akt levels showed similar trends to total eNOS; KO PECs show a negative correlation between VEGF concentration and total Akt levels whereas M3 treated PECs show a nominal increase.

Overall, these findings suggest chronic BACE1 inhibition may cause a change in general protein expression of signalling factors involved in angiogenesis, whereas acute BACE1 inhibition does not. This could propose that BACE1 may have a regulatory role in protein expression of angiogenic signalling factors. However, due to the low sample number resulting from the Covid-19 pandemic, these findings must be further explored.

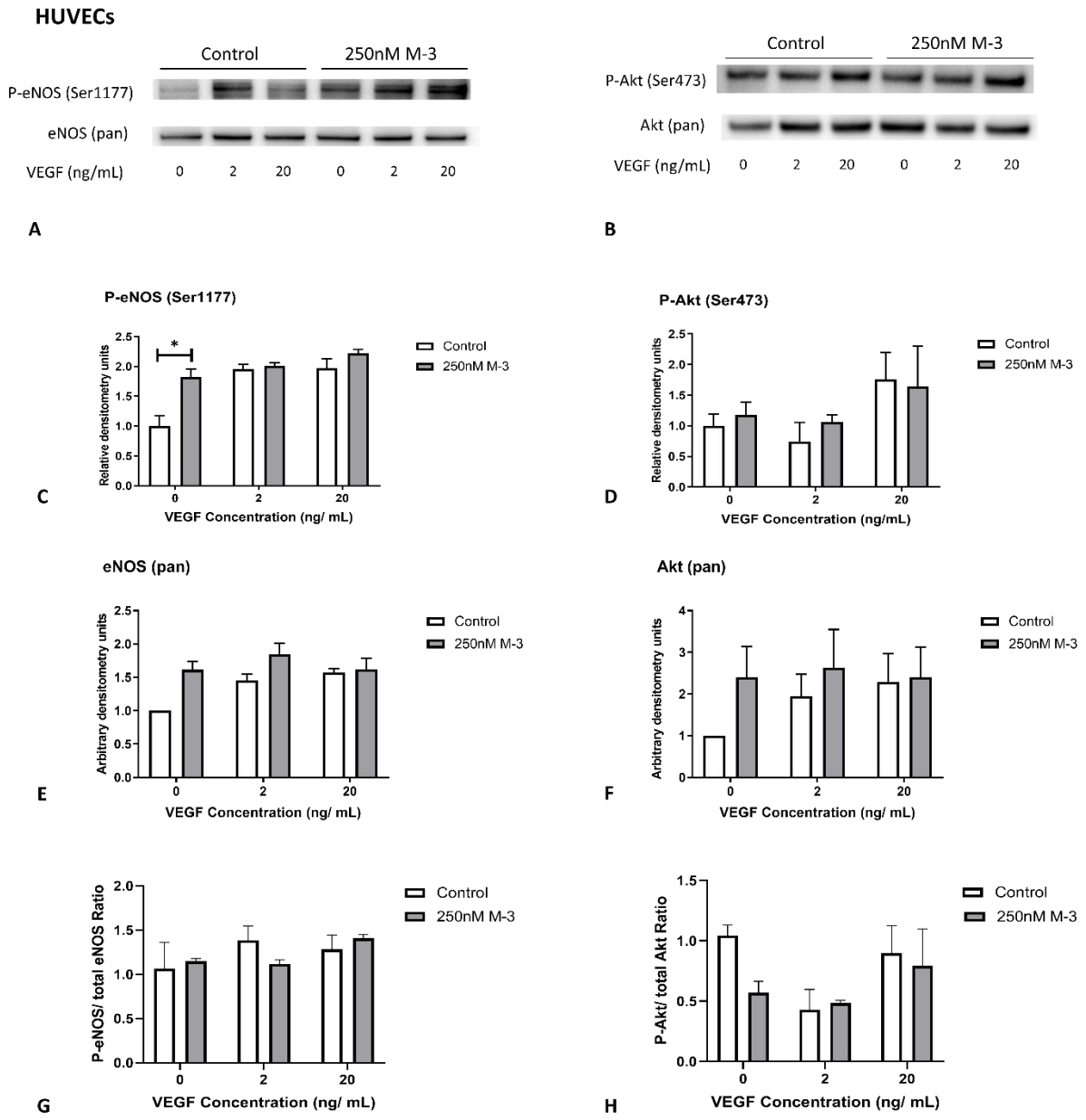
HUVECs
Control
250nM M-3
P-eNOS (Ser1177)
eNOS (pan)
VEGF (ng/mL)
0 2 20 0 2 20
A
Control
250nM M-3
P-Akt (Ser473)
Akt (pan)
VEGF (ng/mL)
0 2 20 0 2 20
B
P-eNOS (Ser1177)
Relative densitometry units
VEGF Concentration (ng/ mL)
Control
250nM M-3
C
P-Akt (Ser473)
Relative densitometry units
VEGF Concentration (ng/mL)
Control
250nM M-3
D
eNOS (pan)
Arbitrary densitometry units
VEGF Concentration (ng/ mL)
Control
250nM M-3
E
Akt (pan)
Arbitrary densitometry units
VEGF Concentration (ng/ mL)
Control
250nM M-3
F
P-eNOS/ total eNOS Ratio
VEGF Concentration (ng/ mL)
Control
250nM M-3
G
P-Akt/ total Akt Ratio
VEGF Concentration (ng/ mL)
Control
250nM M-3
H

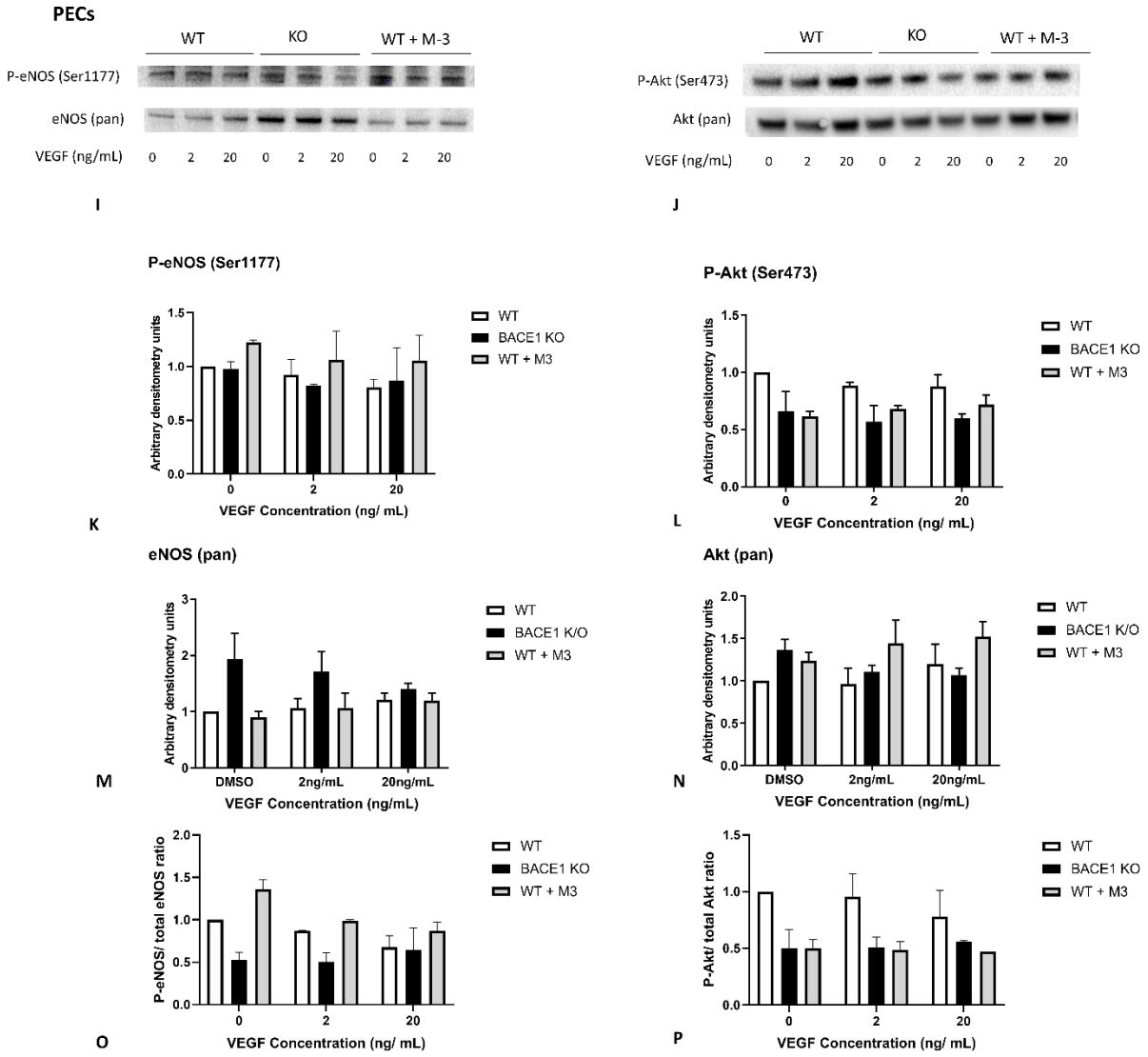

Figure 14: BACE1 inhibition has nominal effects on total levels and phosphorylated activity of eNOS and Akt in HUVECs and PECs A-F) HUVECs (N=3) were treated with 250nM M3 or DMSO (control) then stimulated with either 0ng/mL, 0.5ng/mL or 5.5ng/mL VEGF before their levels of phosphorylated and total eNOS and Akt were analysed by immunoblot. **G)** The ratio of P-eNOS (Ser1177) to total eNOS (pan). **H)** The ratio of P-Akt (Ser473) to total Akt (pan). **I-N)** BACE1 KO, WT (control) and WT + 250nM M3 treated PECs (N=2) were stimulated with 0ng/mL, 0.5ng/mL or 5.5ng/mL VEGF before their levels of phosphorylated and total eNOS and Akt were analysed by immunoblot. **O)** The ratio of P-eNOS (Ser1177) to total eNOS (pan). **P)** The ratio of P-Akt (Ser473) to total Akt (pan). Data are means ± SEM. Statistical analyses were made using unpaired T-tests. *$p < 0.05$.

These results suggest that BACE1 inhibition could have a role in angiogenic sprouting through the regulation of activity of downstream signalling factors. However, the minimal increase shown during VEGF stimulations suggests that M3 utilises an alternative mechanism to increase VEGF-induced sprouting. NOTCH1 signalling is also a key regulator of angiogenic sprouting. Therefore, investigation into the role of BACE1 in NOTCH1 signalling was initiated.

3.6 BACE1 deficient mice have reduced NOTCH1 signalling

Since NOTCH1 signalling is important in tip and stalk cell differentiation, immunoblots for Notch Intracellular Domain 1 (NICD1) were performed on BACE1 KO and WT PECs treated with 250nM M3 or DMSO (Kofler *et al*., 2011). Results of their ADU values displayed a visible decrease in NICD1 levels in BACE1 KO PECs (-0.3100 ± 0.2701 decrease), indicating a potential role of BACE1 in NOTCH signalling (Figures 15A-B). In contrast, WT PECs treated with 250nM M3 showed no significant difference in NICD concentration (0.1221 ± 0.2016 increase).

Earlier research discovered that NOTCH1 signalling supresses tip cell formation and subsequent sprouting (Hellström *et al*., 2007). Therefore, the reduced NICD1 shown in BACE1 KO coincides with the increased vascular density and reduced elongation presented in the BACE1 KO retinal phenotype.

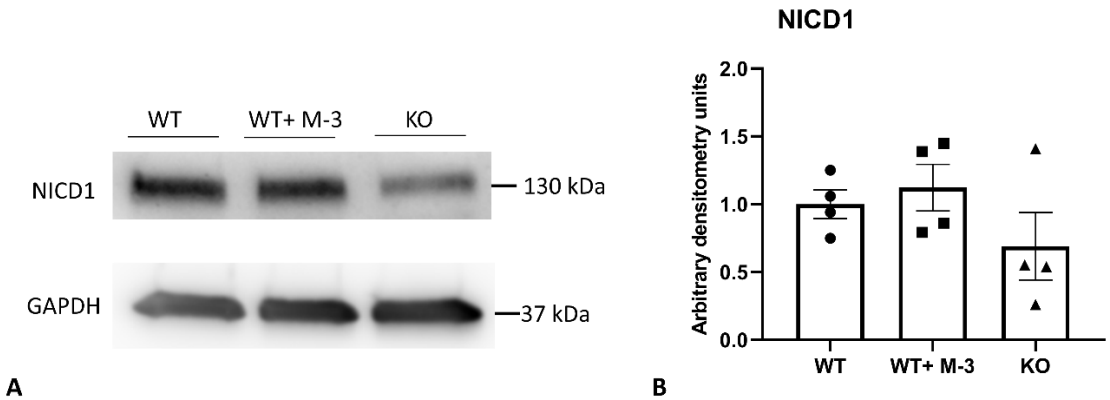

Figure 15: BACE1 deficient mice have reduced NOTCH1 signalling. **A-B)** KO (N=4) and WT PECs +/- 250nM M3 (N=4) were grown to confluency then lysed before their levels of NICD1 were analysed by an immunoblot.

4. Discussion

4.1 General overview

DFUs and lower limb amputations are two debilitating end-stage complications of DM which are associated with increased morbidity and mortality. Thus, to improve the quality and longevity of life in these patients, it is pivotal to prevent such complications from occurring.

This study hypothesises that increased BACE1 levels in DM reduces the angiogenic potential in peripheral vasculature, contributing to the aetiology of DFUs and consequent amputations. This is possibly through BACE1-dependent reduction of VEGF and subsequent VEGFR2-mediated angiogenesis.

The hypothesis was investigated by exploiting *in vivo* and *in vitro* angiogenic models which discovered that BACE1 inhibition generally encouraged angiogenic branching. This was presented by increased pro-angiogenic parameters observed in the retinas of BACE1$^{-/-}$ mice and increased sprouting in a fibrin gel angiogenesis assay using M3-treated HUVECs.

Overall, this project indicates that BACE1 inhibitors may encourage blood vessel growth. This finding could be valuable for the future development of successful therapies targeted to improve angiogenesis and healing in individuals suffering with DFUs.

4.2 Interpretations of results and future experiments

4.2.1 BACE1 deficiency causes altered developmental angiogenesis

Analysis of retinal vasculature stained with IsolectinB4-Alexa-488 in BACE1 $^{-/-}$, BACE1 $^{-/+}$ and WT P5 proved valuable in exploring the role of BACE1 in angiogenesis (Figure 10). The *in vivo* model enabled clear visualisation of endothelial cell composition and analysis of parameters of developmental vessel growth. Results determined that BACE1 deficiency produced a hyper-

branching vascular phenotype. This was shown by the BACE1 $^{-/-}$ mouse exhibiting a decrease in radial outgrowth but an increase in branch points, percentage vasculature area and number of filopodia. Although the BACE1 $^{-/-}$ mouse had a decrease in tip cells, we speculate that this is an anomaly as it is the only measurement that does not conform to the hyper-branching phenotype. Unfortunately, due to the Covid-19 lockdown these parameters were only measured in a single BACE $^{-/-}$ mouse; therefore, this experiment must be repeated to determine its reliability. However, previous investigations by Cai *et al* demonstrate that BACE1-inhibited vessels have a decrease in retinal tubule length and an increase in choroidal neovascularization (CNV) (Cai *et al*., 2012). This supports our results and further confirms that BACE1 inhibition increases vascular branching *in vivo*.

In conjunction with the fibrin gel assay results, we can surmise that BACE1 inhibition encourages endothelial cells to adopt a pro-angiogenic tip cell phenotype, demonstrated though heightened vessel growth. Although our limited *in vivo* images did not demonstrate an increase in tip cells, we speculate that further investigations using confocal microscopy to quantify tip cell production in BACE1$^{-/-}$ and WT mice may possibly do so. Measuring additional tip cell markers, including PFKFB3, in our BACE1 deficient mice could provide an additional insight into the role of BACE1 in tip cell selection.

Moreover, previous research demonstrates that sFlt-1, along with VEGFR1, is predominately secreted by stalk cells, implying that BACE1-dependent Flt-1 proteolysis is attributed to stalk cells (Thalgott *et al*., 2018). However, to determine the precise location of BACE1 in the vasculature front, further investigation must be achieved. Using the retinal staining assay, further analysis for BACE1 can be completed. Visualising BACE1 in WT and diabetic mice models will help determine whether the enzyme is primarily located within tip or stalk cells at the vasculature front and whether it is altered in DM.

Retinal staining is an invaluable experimental system for analysing angiogenesis. Firstly, utilising a whole organism provides a physiological appropriate environment for observing angiogenesis

compared to a singular cell culture (Murphy, 1991). Here, it incorporates a multitude of relevant cells types and factors, providing a comprehensive cellular environment required for vessel growth. Although it is an all-inclusive model for angiogenesis, it decreases the certainty that endothelial cells are the precise variable producing the desired outcome. Therefore, it is essential to also perform *in vitro* experiments on endothelial cells to quantify their activity. Additionally, endothelial-specific $BACE1^{-/-}$ mice will provide an ideal model to observe the role of BACE1 specifically in endothelial cells.

Furthermore, confocal microscopy of the retinal staining enables visualisation of the vessel network in a three-dimensional setting. It can image various important stages of vessel growth at a high resolution, including endothelial cell proliferation, sprouting, perivascular cell recruitment, vessel remodelling and vessel maturation (Pitulescu *et al*.,2010). Comparatively, *in vitro* angiogenic assays performed with single endothelial cell cultures merely display a proportion of these processes. These are also displayed in a two-dimension, proving more difficult to analyse.

The retinal staining experiment, whilst useful to test the role of BACE1 in developmental angiogenesis, was not so relevant in envisioning aberrant angiogenesis occurring in DM. Thus, further *in vivo* experiments, including the hind-limb ischemia model, will be performed in adult diabetic mice models treated with or without M3 (Niiyama *et al*., 2009). This will determine whether BACE1 inhibition will improve peripheral angiogenesis in response to femoral artery ligation, in a more relevant model.

4.2.2 HUVECs are a suitable cell-type for investigating the role of BACE1 *in vitro*

Once it was established that BACE1 has a role in developmental angiogenesis through *in vivo* analysis, it was further investigated using highly manipulated variables *in vitro*. However, to ensure that a suitable endothelial cell type was being used, an immunoblot for BACE1 was performed on a variety of peripheral endothelial cell types (Figure 11). This was necessary as endothelial cells show a

high degree of heterogenicity along the vascular tree depending on their location and immediate microenvironment (Staton, Reed & Brown, 2009). Resultingly, it was discovered that HUVECs contained a substantial quantity of BACE1 in comparison to PECs and SVECs, although this immunoblot experiment must be repeated to confirm its reliability. This is an ideal scenario as HUVECs are easily isolated, due to being successfully cultured since 1973, and are already widely used in angiogenesis assays (Jaffe *et al*., 1973 and Staton, Reed & Brown, 2009). Furthermore, the abundancy of BACE1 in HUVECs implies that the cell type can be easily manipulated with BACE1 inhibitors in comparison to other cell types. However, it must be acknowledged that this immunoblot merely reflects the protein content, and not the extent of its activity.

Notably, HUVECs are isolated from a macrovascular vessel, whereas this project is specifically interested in angiogenesis occurring in microvasculature, explicitly where DFUs are most prominent. Primary Human Dermal Microvascular Endothelial Cells (HDMEC) or primary isolated endothelial cells from diabetic patients may provide more relevant endothelial cell models for our study.

The BACE1 immunoblot also elucidated that primary isolated PECs were suitable for this investigation. WT PECs had sufficient quantities of BACE1, whereas KO PECs were completely deficient, confirming their genotype.

4.2.3 BACE1 inhibition increases angiogenic sprouting in HUVECs

HUVECs were utilised *in vitro* to intricately study the role of BACE1 in angiogenesis. *In vitro* experiments are particularly beneficial because they are much cheaper, highly reproducible and do not involve harming mice. The fibrin gel angiogenesis assay exploited in this project is favourable because it recapitulates early stages of endothelial sprout formation; with nascent vessels displaying intercellular lumens bordered by polarized endothelial cells.

Firstly, two different concentrations of β-Secretase Inhibitor IV (M3), 250nM and 1µM, were used to investigate the concentration required for optimal vessel growth. Results presented that 250nM M3

significantly increased sprout formation by 17% at a normal physiological glucose concentration, whereas 1µM M3 application was much less effective (Figure 12). Notably, M3 is highly specific, having an IC50 of 15nM for BACE1 but an IC50 of 0.23 µM, 7.6 µM and >50 µM for BACE-2, cathepsin D, and renin, respectively. Hence, this may justify why lower concentrations of M3 are more effective; as non-specific inhibition of other enzymes is prevented.

Additionally, BACE1 inhibition showed a significant increase in sprouting; however, much like the *in vivo* findings, there was no effect on sprout elongation. This further supports our theory that BACE1 inhibition promotes tip cell selection, rather than proliferative activities of stalk cells.

Diabetic conditions were modelled by incubating the fibrin clot in a 30mM glucose concentration, simulating hyperglycaemia. Although 30mM is an extremely exaggerated glucose concentration, as a diabetic would usually endure ranges between 7mM-11mM, it will ensure that high levels or glucose can perfuse into the clots to influence their physiology. Additionally, 30mM and 5mM glucose concentrations have formerly been used *in vitro* to investigate hyperglycaemia in comparison to non-diabetic glucose levels (Cagliero *et al*., 1995). Previous research has shown that high glucose concentrations leads to a reduced angiogenic potential in endothelial cells due to altered proliferation, apoptosis and cell cycle progression, occurring principally through the TGF-β1 autocrine pathway (McGinn *et al*., 2003). Thus, providing an ideal diabetic model for this assay. Unfortunately, in this project, a reduced angiogenic potential was not presented at a 30mM glucose concentration, prior to M3 treatment. Such results may be explained by our brief incubation duration, as previous researchers exposed cells to high glucose concentrations for longer periods of time (7- 14 days). Moreover, Esposito *et al* found that exposure of high glucose concentrations to endothelial cells for under 48 hours *increased* proliferation potential, further providing an explanation to our perplexing results (Esposito *et al*., 2001). Nevertheless, elevated glucose concentrations alone are not a perfect model of diabetes, as there are numerous other factors contributing to the disease. Therefore, a more suitable cellular DM model for this particular project

will be to over-express BACE1 in HUVECs using a recombinant over-expression plasmid. This will allow us to observe whether increased BACE1 expression specifically contributes to the reduced angiogenic potential observed in DM.

Results of this assay also demonstrated that the possible effects of BACE1 inhibition on sprouting potential may have been eradicated in extremely high glucose concentrations. Previously, it has been shown that along with cellular stressors mentioned in the introduction, high glucose concentrations can upregulate BACE1 activity through various mechanisms including ROS dependent HIF-1 production and lipid raft reorganisation (Lee *et al*., 2016). Therefore, if BACE1 levels are increased in the 30mM glucose concentration condition, the 250nM M3 activity may no longer be sufficient to counteract its increased activity, providing an equitable explanation for these findings.

The fibrin gel angiogenesis assay was invaluable in investigating tip cell selection, sprout migration and endothelial proliferation in HUVECs subjected to M3 treatment. However, this experimental technique also has its disadvantages. Firstly, the assay does not consider the roles of other cell types involved in angiogenesis, including pericytes, SMCs, ECM components. Therefore, the *in vitro* model cannot be considered a comprehensive insight into angiogenesis, which must be accounted for when interpreting results. Secondly, the assay does not display all aspects of angiogenesis including sprout anastomosis or vessel maturation; two essential processes for achieving structurally functioning vessels. Using the *in vivo* retinal staining experiment, these parameters can be observed. Previous work by Cai *et al* has identified vessel abnormalities in BACE1 $^{-/-}$ retinas such as loss of pericytes and retinal thinning (Cai *et al*., 2012). This data could suggest that BACE1 inhibition potentially encourages improper vascular growth, causing other complications. Further investigation must be performed to ensure this is not the case.

Notably, only one BACE1 inhibiting compound has been investigated in this project. Therefore, it cannot be certain whether the hyper-sprouting effects we tended to see *in vitro* are the consequence of BACE1 inhibition or the off-target effects of M3. Further experimentation using

alternative BACE1 inhibiting drugs or other protein silencing techniques are required to ensure experimental validity.

4.2.4 BACE1 inhibition increases sprout formation through VEGF signalling

To investigate whether BACE1 inhibition effected VEGF signalling, we performed the fibrin gel angiogenesis assay with varying concentrations of supplementary VEGF (Figure 13). Our results demonstrated that increased VEGF levels enhanced M3 responses, shown particularly through the percentage increase in sprout number succeeding M3 treatment. Additionally, similar to previous findings, VEGF levels had no effect on the influence of M3 on sprout length, again supporting the theory that BACE1 inhibition specifically effects sprout initiation processes.

Notably, this project initially hypothesised that BACE1 inhibition increases VEGF bioavailability by preventing the proteolysis of Flt-1 to sFlt-1. Therefore, increased VEGF levels in BACE1 inhibited cells may cause the system to have surplus VEGF due to deficient antagonistic sFlt-1; proposing that supplementary VEGF should not influence sprouting. Our results oppose this proposition which suggests that BACE1 inhibition effects angiogenic sprouting irrespective of VEGF bioavailability. However, until sFlt-1 levels in the system are quantified, it is uncertain that this variable is negatively regulating angiogenic sprouting. Cai *et al* discovered that sFlt-1 levels were not affected by BACE1 inhibition, supporting the idea M3 may have an alternative mode of pro-angiogenic action (Cai *et al*., 2012).

To ultimately derive whether BACE1 inhibition affects VEGF bioavailability, a negative control experiment using VEGF neutralising antibodies must be performed. This will determine whether VEGF is the predominant factor initiating sprouting and thus being affected by BACE1 inhibition. It will also be imperative to investigate FGF availability, as this growth factor has been used alongside VEGF throughout the fibrin gel angiogenesis assays.

4.2.5 BACE1 inhibition has nominal effects on signalling factors downstream of VEGFR2

Once it was elucidated that BACE1 inhibition and deficiency tended to cause a hyper-branching phenotype both *in vivo* and *in vitro*, the potential mechanism fuelling this was investigated. The initial hypothesis surmises that BACE1 inhibition increases VEGF bioavailability and subsequent VEGFR2 signalling. This was explored in HUVECs and PECs by measuring phosphorylation events of Akt and eNOS, two downstream signalling factors of VEGFR2, following a 30-minute VEGF stimulation (Figure 14).

HUVECs treated with M3 showed an increase in both p-Akt and p-eNOS, which was particularly noticeable for p-eNOS at basal levels (0 ng/mL VEGF). This may suggest that M3 treatment increases p-eNOS levels independent of VEGFR2 stimulation. Interestingly, Meakin *et al* also identified this increase in p-eNOS levels when observing BACE1 inhibition regarding insulin signalling, reinforcing the reliability of our finding (Meakin *et al*., 2018). Aforementioned, BACE1 was found to cleave the insulin receptor; a key protein involved in the phosphorylation of eNOS. Therefore, increased levels of p-eNOS in BACE1 inhibited cells may be attributed to increased insulin receptor signalling rather than VEGFR2 activity. To clarify whether BACE1 inhibition increases VEGFR2 activation specifically, an immunoblot for the VEGFR2 Tyr1175 phosphorylation site must be achieved.

Surprisingly, unlike p-eNOS, p-Akt is only slightly increased in BACE1 inhibited HUVECs. This may suggest that p-eNOS^{1177} is phosphorylated by alternative kinases to Akt. This is plausible as the eNOS s1177 site can be phosphorylated by a broad array of kinases including Protein Kinase A (PKA), AMP-activated protein kinase (AMPK) and CaM kinase II (Eroglu *et al*., 2019; Chen *et al*., 1999 and Fleming *et al*., 2001). Interestingly, AMPK, which is also involved in eliciting insulin-sensitizing effects, is dysregulated in DM models (Coughlan *et al*., 2014). This may suggest that BACE1 is involved is dysregulating AMPK activity and that BACE1 inhibition can reverse this affect, resulting in increased eNOS phosphorylation. Therefore, future experiments exploring AMPK levels in HUVECs treated with or without M3 may be useful.

Increasing VEGF stimulations caused p-eNOS levels to rise systematically in both conditions. This clarifies that a 30-minute VEGF stimulation is an optimal timeframe for eNOS in HUVECs, which has also been proven by previous researchers (Garrett, Van Buul & Burridge, 2007 and Boeldt *et al*., 2017). Although the timeframe seems optimal for investigating phosphorylation events for eNOS in HUVECs, observations other factors, such as VEGFR2, will require a shorter VEGF stimulation time due to their position earlier in the signalling pathway.

Notably, the significant increase of p-eNOS between M3 treated and control HUVECs, shown at 0ng/mL VEGF, did not persist with VEGF stimulations. This arose various interpretations. Firstly, in accordance with the original hypothesis that BACE1 inhibition increases VEGF bioavailability, VEGFR2's may be saturated at basal levels in M3-treated cells. Resultingly, supplementary VEGF cannot have an additional effect (Figure 16). Alternatively, M3 treatment may increase p-eNOS levels through an alternative mechanism to VEGFR2 signalling, thus VEGF stimulations will be ineffective.

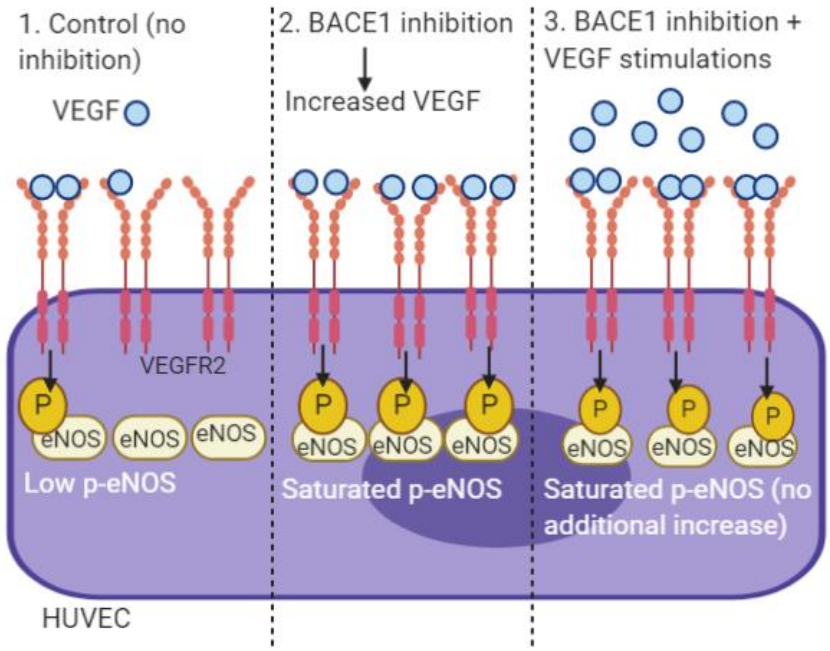

Figure 16: A schematic diagram presenting the above interpretations for the p-eNOS Western blot results. At 0ng/mL VEGF in M3-treated HUVECs, VEGF may be increased to a level which saturates p-eNOS. Therefore,

additional VEGF from stimulations appear to have no additional effect. Alternatively, another mechanism of BACE1-inhbition may increase p-eNOS levels, hence VEGF stimulations being ineffective.

Interestingly, this result contradicts our previous findings presented in the fibrin gel angiogenesis assay. The former assay demonstrated that increased VEGF stimulation in M3-treated HUVECs caused an increase in sprout number, suggesting that the M3 potentiates the pro-sprouting effect of VEGF. However, this assay shows that the pro-angiogenic p-eNOS levels in M3-treated HUVECs are irresponsive to VEGF stimulations. Therefore, investigations into alternative VEGFR2 downstream signalling factors, such as ERK, may provide a useful insight into this query.

Observations of phosphorylated to total protein ratios in HUVECs show perplexing results for both eNOS and Akt. Both results contradict data regarding just the phosphorylated protein. For example, the p-eNOS to total eNOS ratio does not display a significant difference between the two conditions, previously shown in p-eNOS blot. Also, the slight increase in p-Akt in M3 treated HUVECs is not portrayed in the p-Akt to total Akt ratio. Although it is valuable to take this ratio into account, there are numerous problems which can arise from this analysis. For example, the total and phosphorylated proteins were run on separate gels, and even though they have been normalised to a loading control, it is not certain whether the protein loading is accurate or that the antibodies work identically. Therefore, it may be useful to use a more quantitative methods to analyse downstream factors of VEGFR2 signalling, such as an eNOS activity assay.

VEGF stimulations in PECs were particularly useful in comparing chronic BACE1 deficiency in BACE1$^{-/-}$ mice to acute BACE1 inhibition in M3-treated WT mice. Unfortunately, due to time constraints proceeding the Covid-19 pandemic, this experiment was only repeated twice. Therefore, there is insufficient data to test for statistical significance. Unlike HUVECs, it was apparent that the 30-minute time frame used for the VEGF stimulations was not suitable. This is shown by the absence of a sequential positive correlation between phosphorylation events and VEGF concentrations in WT

PECs. Therefore, the precise time frame for measuring p-eNOS and p-Akt levels in WT PECs should be obtained prior to further analysing peak downstream phosphorylation events in BACE1 inhibited and deficient PECs.

In accordance with the HUVEC data, p-eNOS was increased at basal levels in WT PECs treated with M3, which was especially evident in the p-eNOS to total eNOS ratio. This finding could suggest that acute/partial BACE1 inhibition is more effective in activating eNOS compared to chronic/complete BACE1 deficiency. Furthermore, the dramatic increase in total eNOS levels in BACE1$^{-/-}$ cells may suggest that BACE1 deficiency or long-term inhibition increases protein expression of eNOS. However, these remarkable findings must be reproduced to prove their reliability.

Both BACE1 inhibition and deficiency reduces Akt phosphorylation, a finding especially shown by the p-Akt to total ratio. This could be due to total Akt levels increasing with BACE1 inhibition and deficiency, also proposing that BACE1 inhibition can increase protein expression of Akt.

To conclude, BACE1 inhibition notably increases p-eNOS but not p-Akt at basal levels; a finding demonstrated in two endothelial cell models. Moreover, increasing VEGF stimulations did not enhance p-eNOS levels. Therefore, future experiments will focus on determining precisely how BACE1 inhibition increases p-eNOS. To elucidate whether this is the result of BACE1-dependent cleavage of VEGFR1, we will perform cleavage site-mutation experiments. Here, we postulate that cells with mutated VEGFR1 will be unaffected by BACE1 inhibition and that p-eNOS levels will remain analogous to relevant controls.

4.2.6 BACE1 deficient mice have reduced NOTCH1 signalling

Due to the hyper-sprouting phenotype shown *in vitro* and *in vivo*, and the ambiguous VEGF stimulation results, the investigation diverged to examine NOTCH1 signalling. Aforementioned, NOTCH1 is a key receptor for generating a stalk cell phenotype in a nascent sprout. Zheng *et al*

discovered that individuals and mouse models with diabetes had increased NICD1 levels in their skin epidermis; contributing to defective wound healing (Zheng *et al*., 2019). Therefore, if BACE1 inhibition is thought to increase the tip cell phenotype as previously hypothesised, then reduced NOTCH1 signalling would be apparent.

To investigate this, an immunoblot for the NICD1 was performed on PECs (Figure 15). As anticipated, BACE1 deficient cells showed a dramatic reduction in the NICD1, suggesting that this may be the cause of the hyper-sprouting. However, M3 treated WT PECs showed no obvious difference in NICD1 levels. This may suggest that long term or complete BACE1 inhibition was only effective in reducing NICD1 in PECs. Although these results conflict with the M3 treated HUVECs which show a hyper-sprouting phenotype in the fibrin gel angiogenesis assay, this may be because it is a different cell type. Therefore, it will be useful to look at NICD1 levels in BACE1 deficient/ inhibited HUVECs and see whether BACE1 inhibition with M3 also reduces NICD1 in this cell type.

Previous research by Durrant *et al* has also looked at the role of BACE1 and Aβ products in vessel growth (Durrant *et al*., 2020). Although the researchers found contradictory results to this project, they further supported that BACE1 has a role in angiogenesis. Using organotypic brain slice cultures (OBSCs) from a human-APP transgenic mouse (TgCRND8) model, they found that increased Aβ processing by BACE1 caused hyper-sprouting. This is thought to be through the dysregulation of NOTCH3/JAG1 signalling, which also supports our recent assumption that BACE1 effects NOTCH signalling. However, this research primarily focussed on NOTCH3 signalling, a receptor we have not yet looked at in our BACE1$^{-/-}$ model.

Although the results of Durrant *et al* predominantly contradict ours, there are numerous potential reasons for this. Firstly, the organotypic brain slice cultures (OBSCs) differs from the mouse retinal staining model exploited in our investigation. OBSCs focus on vasculature within the brain which has a distinctive cellular environment compared to the retinal vasculature. Furthermore, the OBSCs are subjected to exceptional injury during the slicing procedure. Therefore, the system encourages

angiogenesis through cellular damage and hypoxia rather than developmental VEGF dependent vessel growth.

Whilst we hypothesise that BACE1 inhibition increases angiogenesis through VEGF bioavailability, we cannot ignore the effects of Aβ in this process. Previous research has demonstrated that Aβ42 production in the brain causes endothelial dysfunction through reducing NO levels (Meakin *et al*., 2020). However, the brain has increased BACE1 activity and Aβ production, suggesting that here BACE1 activity may have differing effects to the rest of the body.

Finally, Durrant *et al* used an alternative BACE inhibitor, LY2886721, which is also extremely potent at inhibiting BACE2. Therefore, it is unsurprising that the effects seen in response to LY2886721 differs from M3, a highly specific BACE1 inhibitor. Repeating our chosen angiogenesis assays using LY2886721 will be valuable to observe whether the inhibitor has dissimilar effects on sprouting to M3. Notably, it has been proven that inhibiting BACE1 *and* BACE2 has more severe and detrimental effects to inhibiting either one, demonstrated by lethality in BACE1 and BACE2 null mice. This is because the proteases can compensate slightly for each other (Dominguez *et al*., 2005).

4.3 Possible alternative hypothesis

Earlier investigations discovered that Jagged-1 (Jag1), a NOTCH1 ligand, is cleaved by BACE1 between residues Ala^{1050}-Ala^{1051} to release a soluble ectodomain (sJag1) (He *et al*., 2014). The remaining C-terminus fragment is subsequently cleaved by the γ-secretase complex, similarly to APP proteolysis, to further release an intracellular domain (Jag1-ICD) which is found to upregulate Jag1 expression (Azimi & Brown, 2019).

Pro-angiogenic Jag1 is expressed predominately on stalk cells and plays a role in negatively regulating NOTCH1 signalling in neighbouring tip cells. This is done through antagonizing Dll4-induced NOTCH1 activation, decreasing NOTCH1 expression and increasing NOTCH4 expression, a

receptor involved in cis-inhibition of NOTCH1 signalling (Suchting & Eichmann, 2009; James *et al*., 2014 and Pedrosa *et al*., 2015). Additionally, Kangsamaksin *et al* discovered that Jag1/NOTCH1 signalling between tip and stalk cells reduces sFlt-1 expression, increasing VEGF bioavailability important in preserving the tip cell phenotype (Kangsamaksin *et al*., 2015). This could suggest that the decrease in sFlt-1 levels observed in BACE1$^{-/-}$ mice may be an indirect product of BACE1-depedent proteolysis of Jag1 rather than of Flt-1, although this must be further explored.

Furthermore, Benedito *et al* discovered that the retinas of mice which are genetically induced to over-express Jag1 had a similar hyper-sprouting phenotype to the BACE1$^{-/-}$ mouse shown in our results (Benedito *et al*., 2009). This insinuates that BACE1 deficiency increases levels of full-length Jag1 which subsequently reduces sFlt-1 levels, shown in the preliminary data of BACE1 inhibited cells. Moreover, if BACE1 deficiency increases full-length Jag1, then this will outcompete Dll4/NOTCH1 signalling, leading to decreased NICD1 levels which supports our current findings.

If these predictions are accurate, they suggest that the products of BACE1-dependent proteolysis of Jagged-1, sJag1 and Jag-ICD, are anti-angiogenic through the manipulation of NICD1 signalling. This is supported by Pelullo *et al* who showed that sJag1 causes paracrine amplification of NOTCH1 signalling in adjacent cells by upregulating specific NOTCH1 target genes (Pelullo *et al*., 2014).

Contrastingly, during Jag1/NOTCH1 juxtracrine signalling, Jag1-ICD is released. The Jag1-ICD has been found to accelerate the degradation of NICD1 via the Fbw7-dependent proteasomal pathway (Kim *et al*., 2011). Thus, full-length Jag1 (and not sJag-1) may be required for the degradation of NICD1, potentially explaining the low NICD1 seen in our BACE1-deficient mice. Notably, if the JAG1-ICD produced during BACE1 proteolysis also exhibits this activity, it may be insignificant due to its inability to overcome the high proportion of NICD1 produced in stalk cells.

In conclusion, BACE1 inhibition may possibly reduce anti-angiogenic Dll4/NOTCH1 signalling and increase pro-angiogenic Jag1/NOTCH1 signalling; inducing a tip cell phenotype (Figure 17). This could be due to decreased levels of anti-angiogenic spice variant sFlt-1 expression and decreased

production of NICD1, which prevents the formation of a tip cell phenotype. Therefore, BACE1-dependent cleavage of Jag1 may also provide a plausible explanation to the pro-angiogenic characteristics shown in BACE1-deficient mice and BACE1- inhibited HUVECs.

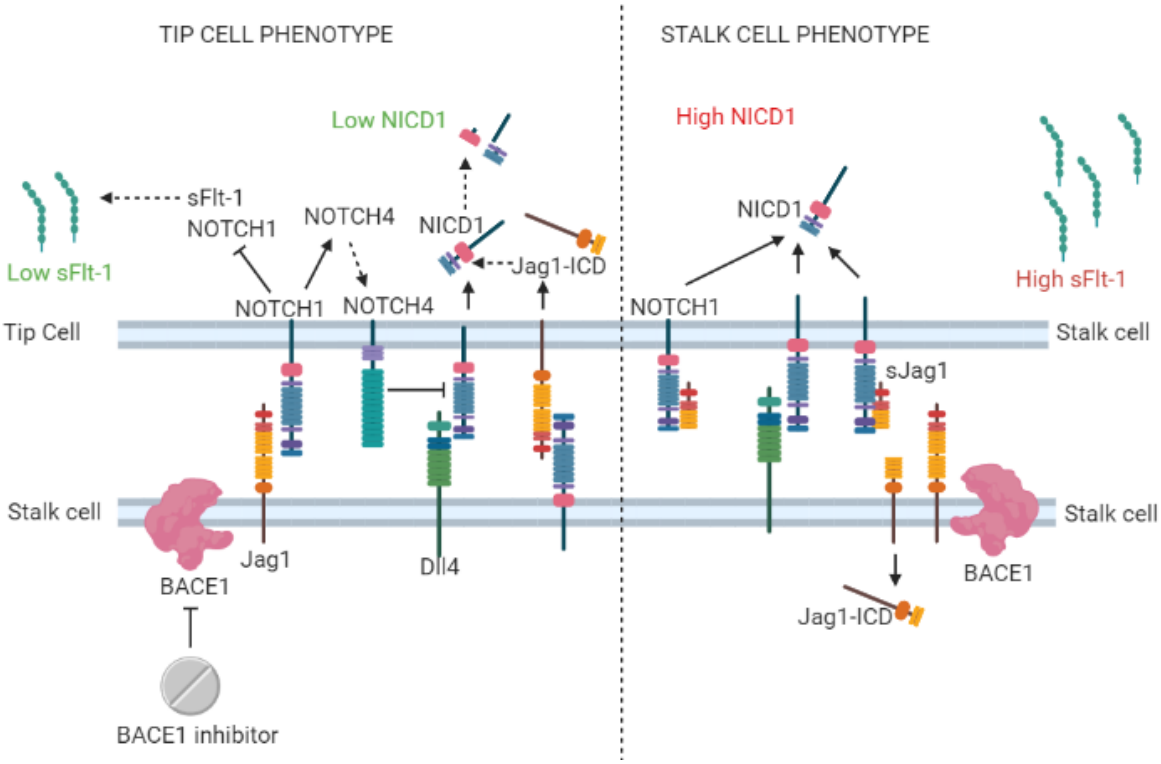

Figure 17: A schematic diagram presenting a potential alternative hypothesis for the role of BACE1 in angiogenesis. It is hypothesised that the hyper-sprouting phenotype presented throughout the study may be the result of BACE1 dependent cleavage of Jag1. This cleavage reduces pro-angiogenic NOTCH1/jag1 signalling and increases anti-angiogenic Dll4/NOTCH1 signalling which subsequently prohibits a tip-cell phenotype. Inhibition of Jag1 proteolysis leads to a decrease in anti-angiogenic sFlt-1 and NICD, causing a pro-angiogenic tip-cell phenotype.

In support of this hypothesis, diabetic models were found to have increased Dll4 expression which resulted in the upregulation of anti-angiogenic Dll4/NOTCH1 signalling. Although the researchers elucidated that hyperglycaemia was the predominant factor of DM triggering this, our hypothesis provides an alternative mechanism: BACE1-dependent cleavage of Jag1 reduces Jag1/NOTCH1 signalling, thereby encouraging Dll4/NOTCH1 signalling.

4.4 Conclusion

Understanding the role of BACE1 in peripheral angiogenesis could provide novel therapeutic insights into treating poor angiogenesis present in DFUs. Consequently, this may prevent debilitating lower limb amputations from occurring. This study has suggested that BACE1 reduction can encourage angiogenesis both *in vivo* and *in vitro* models. Although we originally hypothesised that this was the consequence of increased VEGF and subsequent VEGFR2 signalling, our results suggest it may be attributed to alternative mechanisms which are still yet to be elucidated. However, not only does this report state our revised hypotheses, it outlines various suggestions to investigate these in the future. Overall, this project is significant as it suggests that BACE1 inhibiting drugs can potentially be repurposed to prevent microvascular complications and improve the health and longevity of individuals with DM.

5. References

Amano, H., Kato, S., Ito, Y., Eshima, K., Ogawa, F., Takahashi, R., Sekiguchi, K., Tamaki, H., Sakagami, H., Shibuya, M., & Majima, M. (2015). The role of vascular endothelial growth factor receptor-1 signaling in the recovery from ischemia. *PLoS ONE*. **10**(7), pp. e0131445.

Andreeva, N. S., & Rumsh, L. D. (2001). Analysis of crystal structures of aspartic proteinases: on the role of amino acid residues adjacent to the catalytic site of pepsin-like enzymes. *Protein Science*. **10**(12), pp. 2439-2450.

Azimi, M., & Brown, N. L. (2019). Jagged1 protein processing in the developing mammalian lens. *Biology Open*. **8**(3).

Barman, A., & Prabhakar, R. (2014). Computational Insights into Substrate and Site Specificities, Catalytic Mechanism, and Protonation States of the Catalytic Asp Dyad of β-Secretase. *Scientifica*. **2014**, pp. 1-11.

Barrientos, S., Stojadinovic, O., Golinko, M. S., Brem, H., & Tomic-Canic, M. (2008). Growth factors and cytokines in wound healing. *Wound Repair and Regeneration*. **16**(5), pp. 585-601.

Baumgartner, I., Pieczek, A., Manor, O., Blair, R., Kearney, M., Walsh, K., & Isner, J. M. (1998). Constitutive expression of phVEGF165 after intramuscular gene transfer promotes collateral vessel development in patients with critical limb ischemia. *Circulation*. **97**(12), pp. 1114–1123.

Benedito, R., Roca, C., Sörensen, I., Adams, S., Gossler, A., Fruttiger, M., & Adams, R. H. (2009). The Notch Ligands Dll4 and Jagged1 Have Opposing Effects on Angiogenesis. *Cell*. **137**(6), pp. 1124-1135.

Benjannet, S., Elagoz, A., Wickham, L., Mamarbachi, M., Munzer, J. S., Basak, A., Lazure, C., Cromlish, J. A., Sisodia, S., Checler, F., Chrétien, M., & Seidah, N. G. (2001). Post-translational processing of beta-secretase (beta-amyloid-converting enzyme) and its ectodomain shedding. The pro- and transmembrane/cytosolic domains affect its cellular activity and amyloid-beta production. *The Journal of Biological Chemistry*. **276**(14), pp. 10879–10887.

Bennett, B. D., Denis, P., Haniu, M., Teplow, D. B., Kahn, S., Louis, J. C., Citron, M., & Vassar, R. (2000). A furin-like convertase mediates propeptide cleavage of BACE, the Alzheimer's β-secretase. *Journal of Biological Chemistry*. **275**, pp. 37712-37717

Betz, C., Lenard, A., Belting, H. G., & Affolter, M. (2016). Cell behaviors and dynamics during angiogenesis. *Development*. **143**, pp. 2249-2260.

Blanco, R., & Gerhardt, H. (2013). VEGF and Notch in tip and stalk cell selection. *Cold Spring Harbor Perspectives in Medicine*. **3**(1), pp. a006569–a006569.

Boeldt, D. S., Krupp, J., Yi, F.-X., Khurshid, N., Shah, D. M., & Bird, I. M. (2017). Positive versus negative effects of VEGF165 on Ca2+ signaling and NO production in human endothelial cells. American Journal of Physiology. *Heart and Circulatory Physiology*. **312**(1), pp. H173-H181.

Broadhead, M. L., Becerra, S. P., Choong, P. F. M., & Dass, C. R. (2010). The applied biochemistry of PEDF and implications for tissue homeostasis. *Growth Factors*. **28**(4), pp. 280-285.

Brown, R. L., Breeden, M. P., & Greenhalgh, D. G. (1994). PDGF and TGF-α act synergistically to improve wound healing in the genetically diabetic mouse. *Journal of Surgical Research*. **56**(6), pp. 562-570.

Burdick, D., Soreghan, B., Kwon, M., Kosmoski, J., Knauer, M., Henschen, A., Yates, J., Cotman, C., & Glabe, C. (1992). Assembly and aggregation properties of synthetic Alzheimer's A4/beta amyloid peptide analogs. *The Journal of Biological Chemistry*. **267**(1), pp. 546–554.

Cagliero, E., Roth, T., Taylor, A. W., & Lorenzi, M. (1995). The effects of high glucose on human endothelial cell growth and gene expression are not mediated by transforming growth factor-beta. *Laboratory Investigation; a Journal of Technical Methods and Pathology*. **73**(5), pp. 667-673.

Cai, J., Qi, X., Kociok, N., Skosyrski, S., Emilio, A., Ruan, Q., Han, S., Liu, L., Chen, Z., Bowes Rickman, C., Golde, T., Grant, M. B., Saftig, P., Serneels, L., de Strooper, B., Joussen, A. M., & Boulton, M. E. (2012). β-Secretase (BACE1) inhibition causes retinal pathology by vascular dysregulation and accumulation of age pigment. *EMBO Molecular Medicine*. **4**(9), pp. 980–991.

Carmeliet, P. (2003). Angiogenesis in health and disease. *Nature Medicine*. **9**(6): 653-660.

Chami, L., & Checler, F. (2012). BACE1 is at the crossroad of a toxic vicious cycle involving cellular stress and β-amyloid production in Alzheimer's disease. *Molecular Neurodegeneration*. **7**(1), pp. 52.

Chen, C. H., Zhou, W., Liu, S., Deng, Y., Cai, F., Tone, M., Tone, Y., Tong, Y., & Song, W. (2012). Increased NF-κB signalling up-regulates BACE1 expression and its therapeutic potential in Alzheimer's disease. *International Journal of Neuropsychopharmacology*. **15**(1), pp. 77–90

Chen, Z. P., Mitchelhill, K. I., Michell, B. J., Stapleton, D., Rodriguez-Crespo, I., Witters, L. A., Power, D. A., Ortiz De Montellano, P. R., & Kemp, B. E. (1999). AMP-activated protein kinase phosphorylation of endothelial NO synthase. *FEBS Letters*. **443**(3), pp. 285-289.

Chen, Z., Fu, S., Wu, Z., Chen, J., Huang, Y., Wang, Y., & Fu, M. (2018). Relationship between plasma angiogenic growth factors and diabetic foot ulcers. *Clinica Chimica Acta; International Journal of Clinical Chemistry*. **482**, pp. 95–100.

Chereddy, K. K., Lopes, A., Koussoroplis, S., Payen, V., Moia, C., Zhu, H., Sonveaux, P., Carmeliet, P., des Rieux, A., Vandermeulen, G., & Préat, V. (2015). Combined effects of PLGA and vascular endothelial growth factor promote the healing of non-diabetic and diabetic wounds. *Nanomedicine: Nanotechnology, Biology, and Medicine*. **11**(8), pp. 1975-1984

Chuang, P. Y., Yu, Q., Fang, W., Uribarri, J., & He, J. C. (2007). Advanced glycation end products induce podocyte apoptosis by activation of the FOXO4 transcription factor. *Kidney International*. 72(8), pp. 965-976.

Chung, A. S., Lee, J., & Ferrara, N. (2010). Targeting the tumour vasculature: insights from physiological angiogenesis. *Nature Reviews Cancer*. **10**(7), pp. 505–514.

Clegg, L. E., Ganta, V. C., Annex, B. H., & Mac Gabhann, F. (2017). Systems Pharmacology of VEGF165b in Peripheral Artery Disease. *CPT: Pharmacometrics & Systems Pharmacology*. **6**(12), pp. 833-844.

Cole, S. L., & Vassar, R. (2008). The role of amyloid precursor protein processing by BACE1, the β-secretase, in Alzheimer disease pathophysiology. *Journal of Biological Chemistry*. **283**, pp. 29621-29625.

Coleman, D. L. (1978). Obese and diabetes: Two mutant genes causing diabetes-obesity syndromes in mice. *Diabetologia*. **14**, pp. 141–148.

Conway, E. M., Collen, D., & Carmeliet, P. (2001). Molecular mechanisms of blood vessel growth. *Cardiovascular Research*. **49**(3), pp. 507–521.

Cooke. J., & Losordo, D. (2002). Nitric Oxide and Angiogenesis. *Circulation*. **105**(18), pp. 2133–2135.

Coughlan, K. A., Valentine, R. J., Ruderman, N. B., & Saha, A. K. (2014). AMPK activation: A therapeutic target for type 2 diabetes? *Diabetes, Metabolic Syndrome and Obesity: Targets and Therapy*. **2014**(7), pp. 241-253.

De Bock, K., Georgiadou, M., & Carmeliet, P. (2013). Role of endothelial cell metabolism in vessel sprouting. *Cell Metabolism*. **18**(5), pp. 634–647.

Devi, L., Alldred, M. J., Ginsberg, S. D., & Ohno, M. (2012). Mechanisms underlying insulin deficiency-induced acceleration of β-amyloidosis in a mouse model of Alzheimer's disease. *PLoS ONE*. **7**(3), pp. e32792.

Devraj, K., Poznanovic, S., Spahn, C., Schwall, G., Harter, P. N., Mittelbronn, M., Antoniello, K., Paganetti, P., Muhs, A., Heilemann, M., Hawkins, R. A., Schrattenholz, A., & Liebner, S. (2016). BACE-1 is expressed in the blood-brain barrier endothelium and is upregulated in a murine model of Alzheimer's disease. Journal of Cerebral Blood Flow and Metabolism: *Official Journal of the International Society of Cerebral Blood Flow and Metabolism*. **36**(7). pp. 1281–1294.

Dinh, T., & Veves, A. (2005). Microcirculation of the Diabetic Foot. *Current Pharmaceutical Design*. **11**(18), pp. 2301-2309.

Dislich, B., & Lichtenthaler, S. (2012). The Membrane-Bound Aspartyl Protease BACE1: Molecular and Functional Properties in Alzheimer's Disease and Beyond. *Frontiers in Physiology*. **3**, pp. 8.

Dominguez, D., Tournoy, J., Hartmann, D., Huth, T., Cryns, K., Deforce, S., Serneels, L., Camacho, I. E., Marjaux, E., Craessaerts, K., Roebroek, A. J. M., Schwake, M., D'Hooge, R., Bach, P., Kalinke, U., Moechars, D., Alzheimer, C., Reiss, K., Saftig, P., & De Strooper, B. (2005). Phenotypic and biochemical analyses of BACE1- and BACE2-deficient mice. *Journal of Biological Chemistry*. **280**, pp. 30797-30806.

Durrant, C. S., Ruscher, K., Sheppard, O., Coleman, M. P., & Özen, I. (2020). Beta secretase 1-dependent amyloid precursor protein processing promotes excessive vascular sprouting through NOTCH3 signalling. *Cell Death and Disease*. **11**(98).

Duvillié, B., Cordonnier, N., Deltour, L., Dandoy-Dron, F., Itier, J. M., Monthioux, E., Jami, J., Joshi, R. L., & Bucchini, D. (1997). Phenotypic alterations in insulin-deficient mutant mice. *Proceedings of the National Academy of Sciences of the United States of America*. **94**(10), pp. 5137-5140.

Duvillié, B., Cordonnier, N., Deltour, L., Dandoy-Dron, F., Itier, J.-M., Monthioux, E., Jami, J., Joshi, R. L., & Bucchini, D. (1997). Phenotypic alterations in insulin-deficient mutant mice. *Proceedings of the National Academy of Sciences*. **94**(10), pp. 5137-5140.

Eliceiri, B. P., Paul, R., Schwartzberg, P. L., Hood, J. D., Leng, J., & Cheresh, D. A. (1999). Selective Requirement for Src Kinases during VEGF-Induced Angiogenesis and Vascular Permeability. *Molecular Cell*. **4**(6), pp. 915–924.

Eroglu, E., Saravi, S. S. S., Sorrentino, A., Steinhorn, B., & Michel, T. (2019). Discordance between eNOS phosphorylation and activation revealed by multispectral imaging and chemogenetic methods. *Proceedings of the National Academy of Sciences*. **116**(40), pp. 20210-20217.

Escudero, C. A., Herlitz, K., Troncoso, F., Guevara, K., Acurio, J., Aguayo, C., Godoy, A. S., & González, M. (2017). Pro-angiogenic Role of Insulin: From Physiology to Pathology. *Frontiers in Physiology*. **8**, pp. 204.

Esposito, C., Fasoli, G., Plati, A., Bellotti, N., Conte, M. M., Cornacchia, F., Foschi, A., Mazzullo, T., Semeraro, L., & Dal Canton, A. (2001). Long-term exposure to high glucose up-regulates VCAM-induced endothelial cell adhesiveness to PBMC. *Kidney International*. **58**(5), pp. 1842-1849.

Fleming, I., Fisslthaler, B., Dimmeler, S., Kemp, B. E., & Busse, R. (2001). Phosphorylation of Thr(495) regulates Ca(2+)/calmodulin-dependent endothelial nitric oxide synthase activity. *Circulation Research*. **88**(11), pp. E68-75.

Galiano, R. D., Tepper, O. M., Pelo, C. R., Bhatt, K. A., Callaghan, M., Bastidas, N., Bunting, S., Steinmetz, H. G., & Gurtner, G. C. (2004). Topical vascular endothelial growth factor accelerates diabetic wound healing through increased angiogenesis and by mobilizing and recruiting bone marrow-derived cells. *American Journal of Pathology*. **164**(6), pp. 1935-47.

Garrett, T. A., Van Buul, J. D., & Burridge, K. (2007). VEGF-induced Rac1 activation in endothelial cells is regulated by the guanine nucleotide exchange factor Vav2. *Experimental Cell Research*. **313**(15), pp. 3285-3297.

Geudens, I., & Gerhardt, H. (2011). Coordinating cell behaviour during blood vessel formation. *Development*. **138**(21), pp. 4569-4583.

Ghosh, A. K., & Osswald, H. L. (2014). BACE1 (β-secretase) inhibitors for the treatment of Alzheimer's disease. *Chemical Society Reviews*. **43**(19): 6765-6813.

Guglielmotto, M., Aragno, M., Tamagno, E., Vercellinatto, I., Visentin, S., Medana, C., Catalano, M. G., Smith, M. A., Perry, G., Danni, O., Boccuzzi, G., & Tabaton, M. (2012). AGEs/RAGE complex upregulates BACE1 via NF-κB pathway activation. *Neurobiology of Aging*. **33**(1), pp. 196.e13-196.e27.

Hamilton, D. L., Findlay, J. A., Montagut, G., Meakin, P. J., Bestow, D., Jalicy, S. M., & Ashford, M. L. J. (2014). Altered amyloid precursor protein processing regulates glucose uptake and oxidation in cultured rodent myotubes. *Diabetologia*. **57**, pp. 1684–1692.

Hanft, J. R., Pollak, R. A., Barbul, A., van Gils, C., Kwon, P. S., Gray, S. M., Lynch, C. J., Semba, C. P., & Breen, T. J. (2008). Phase I trial on the safety of topical rhVEGF on chronic neuropathic diabetic foot ulcers. *Journal of Wound Care*. **17**(1), pp. 0969-0700

Harrington, L. S., Sainson, R. C. A., Williams, C. K., Taylor, J. M., Shi, W., Li, J.-L., & Harris, A. L. (2008). Regulation of multiple angiogenic pathways by Dll4 and Notch in human umbilical vein endothelial cells. *Microvascular Research*. **75**(2), pp. 144-154.

Harris, R., & Fahrenholz, F. (2005). Alzheimer's Disease: Cellular and Molecular Aspects of Amyloid beta. *Springer US*. **38**, pp. 79-103.

He, W., Hu, J., Xia, Y., & Yan, R. (2014). β-Site amyloid precursor protein cleaving enzyme 1 (BACE1) regulates Notch signalling by controlling the cleavage of Jagged 1 (Jag1) and Jagged2 (Jag2) proteins. *Journal of Biological Chemistry*. **289**, pp. 20630-20637.

Hemming, M. L., Elias, J. E., Gygi, S. P., & Selkoe, D. J. (2009). Identification of β-secretase (BACE1) substrates using quantitative proteomics. *PLoS ONE*. **4**(12), pp. e8477.

Holman, N., Young, R. J., & Jeffcoate, W. J. (2012). Variation in the recorded incidence of amputation of the lower limb in England. *Diabetologia*. **55**(7), pp. 1919–1925.

Hong, L., & Tang, J. (2004). Flap Position of Free Memapsin 2 (β-Secretase), a Model for Flap Opening in Aspartic Protease Catalysis. *Biochemistry*. **43**(16), pp. 4689-4695.

Hong, L., Koelsch, G., Lin, X., Wu, S., Terzyan, S., Ghosh, A. K., Zhang, X. C., & Tang, J. (2000). Structure of the Protease Domain of Memapsin 2 (β-Secretase) Complexed with Inhibitor. *Science*. **290**(5489), pp. 150-153.

Huang, X., Cuajungco, M. P., Atwood, C. S., Hartshorn, M. A., Tyndall, J. D. A., Hanson, G. R., Stokes, K. C., Leopold, M., Multhaup, G., Goldstein, L. E., Scarpa, R. C., Saunders, A. J., Lim, J., Moir, R. D., Glabe, C., Bowden, E. F., Masters, C. L., Fairlie, D. P., Tanzi, R. E., & Bush, A. I. (1999). Cu(II) potentiation of Alzheimer aβ neurotoxicity. Correlation with cell-free hydrogen peroxide production and metal reduction. *Journal of Biological Chemistry*. **274**, pp. 37111-37116.

Hubbard, S. R. (2013). The insulin receptor: both a prototypical and atypical receptor tyrosine kinase. *Cold Spring Harbor Perspectives in Biology*. **5**(3), pp. a008946.

Hussain, I., Powell, D., Howlett, D. R., Tew, D. G., Meek, T. D., Chapman, C., Gloger, I. S., Murphy, K. E., Southan, C. D., Ryan, D. M., Smith, T. S., Simmons, D. L., Walsh, F. S., Dingwall, C., & Christie, G. (1999). Identification of a novel aspartic protease (Asp 2) as β-secretase. *Molecular and Cellular Neurosciences*. **14**(6), pp. 419-427.

Jaffe, E. A., Nachman, R. L., Becker, C. G., & Miinick, C. R. (1973). Culture of Human Endothelial Cells Derived from Umbilical Veins. *The Journal of Clinical Investigation*. **52**, pp. 2745-2756

James, A. C., Szot, J. O., Iyer, K., Major, J. A., Pursglove, S. E., Chapman, G., & Dunwoodie, S. L. (2014). Notch4 reveals a novel mechanism regulating Notch signal transduction. *Biochimica et Biophysica Acta - Molecular Cell Research*. **1843**(7), pp. 1272-1284.

Johnson, J. L., Chambers, E., & Jayasundera, K. (2013). Application of a Bioinformatics-Based Approach to Identify Novel Putative *in vivo* BACE1 Substrates. *Biomedical Engineering and Computational Biology*. **5**.

Kangsamaksin, T., Murtomaki, A., Kofler, N. M., Cuervo, H., Chaudhri, R. A., Tattersall, I. W., Rosenstiel, P. E., Shawber, C. J., & Kitajewski, J. (2015). NOTCH decoys that selectively block DLL/NOTCH or JAG/NOTCH disrupt angiogenesis by unique mechanisms to inhibit tumor growth. *Cancer Discovery*. **5**(2), pp. 182-197.

Kasuga, K., Kaneko, H., Nishizawa, M., Onodera, O., & Ikeuchi, T. (2007). Generation of intracellular domain of insulin receptor tyrosine kinase by γ-secretase. *Biochemical and Biophysical Research Communications*. **360**(1), pp. 90-96.

Kendall, R. L., & Thomas, K. A. (1993). Inhibition of vascular endothelial cell growth factor activity by an endogenously encoded soluble receptor. *Proceedings of the National Academy of Sciences of the United States of America*. **90**(22), pp. 10705-10709.

Kerr, M., Barron, E., Chadwick, P., Evans, T., Kong, W. M., Rayman, G., Sutton-Smith, M., Todd, G., Young, B., & Jeffcoate, W. J. (2019). The cost of diabetic foot ulcers and amputations to the National Health Service in England. *Diabetic Medicine*. **36**(8), pp. 995-1002.

Kikuchi, R., Nakamura, K., MacLauchlan, S., Ngo, D. T.-M., Shimizu, I., Fuster, J. J., Katanasaka, Y., Yoshida, S., Qiu, Y., Yamaguchi, T. P., Matsushita, T., Murohara, T., Gokce, N., Bates, D. O., Hamburg,

N. M., & Walsh, K. (2014). An antiangiogenic isoform of VEGF-A contributes to impaired vascularization in peripheral artery disease. *Nature Medicine*. **20**(12), pp. 1464-1471.

Kim, M.-Y., Jung, J., Mo, J.-S., Ann, E.-J., Ahn, J.-S., Yoon, J.-H., & Park, H.-S. (2011). The intracellular domain of Jagged-1 interacts with Notch1 intracellular domain and promotes its degradation through Fbw7 E3 ligase. *Experimental Cell Research*. **317**(17), pp. 2438–2446.

King, G. L., Buzney, S. M., Kahn, C. R., Hetu, N., Buchwald, S., Macdonald, S. G., & Rand, L. I. (1983). Differential responsiveness to insulin of endothelial and support cells from micro- and macrovessels. *Journal of Clinical Investigation*. **71**(4), pp. 974-979.

Kobayashi, K., Forte, T. M., Taniguchi, S., Ishida, B. Y., Oka, K., & Chan, L. (2000). The db/db mouse, a model for diabetic dyslipidemia: Molecular characterization and effects of western diet feeding. *Metabolism - Clinical and Experimental*. **49**(1), pp. 22-31.

Koelsch, G. (2017). BACE1 Function and inhibition: Implications of intervention in the amyloid pathway of Alzheimer's disease pathology. *Molecules*. **22**(10), pp. 1723.

Kofler, N. M., Shawber, C. J., Kangsamaksin, T., Reed, H. O., Galatioto, J., & Kitajewski, J. (2011). Notch signaling in developmental and tumor angiogenesis. *Genes & cancer*: **2**(12), pp. 1106–1116.

Kolluru, G. K., Bir, S. C., & Kevil, C. G. (2012). Endothelial Dysfunction and Diabetes: Effects on Angiogenesis, Vascular Remodeling, and Wound Healing. *International Journal of Vascular Medicine.* **2012**(918267), pp. 30.

Kota, S. K., Kota, S. K., Meher, L. K., Sahoo, S., Mohapatra, S., & Modi, K. D. (2013). Surgical revascularization techniques for diabetic foot. *Journal of Cardiovascular Disease Research*. **4**(2), pp. 79-83.

Labrecque, L., Royal, I., Surprenant, D. S., Patterson, C., Gingras, D., & Béliveau, R. (2002). Regulation of Vascular Endothelial Growth Factor Receptor-2 Activity by Caveolin-1 and Plasma Membrane Cholesterol. *Molecular Biology of the Cell*. **14**(1), pp. 334-347.

Lamalice, L., Houle, F., Jourdan, G., & Huot, J. (2004). Phosphorylation of tyrosine 1214 on VEGFR2 is required for VEGF-induced activation of Cdc42 upstream of SAPK2/p38. *Oncogene*. **23**(2), pp. 434-445.

Laurent, L., Fabrice, L. B., & Jacques, H. (2007). Endothelial Cell Migration During Angiogenesis. *Circulation Research*. **100**(6), pp. 782-794.

Lee, H. J., Ryu, J. M., Jung, Y. H., Lee, S.-J., Kim, J. Y., Lee, S. H., Hwang, I. K., Seong, J. K., & Han, H. J. (2016). High glucose upregulates BACE1-mediated Aβ production through ROS-dependent HIF-1α and LXRα/ABCA1-regulated lipid raft reorganization in SK-N-MC cells. *Scientific Reports*. **6**, pp. 36746.

Lee, R. J., Springer, M. L., Blanco-Bose, W. E., Shaw, R., Ursell, P. C., & Blau, H. M. (2000). VEGF gene delivery to myocardium: Deleterious effects of unregulated expression. *Circulation*. **102**(8), pp. 898–901.

Leissring, M. A., Murphy, M. P., Mead, T. R., Akbari, Y., Sugarman, M. C., Jannatipour, M., Anliker, B., Müller, U., Saftig, P., & De Strooper, B. (2002). A physiologic signaling role for the γ-secretase-derived intracellular fragment of APP. *Proceedings of the National Academy of Sciences*. **99**(7), pp. 4697-4702.

Li, C., Yu, T., Liu, Y., Chen, X., & Zhang, X. (2015). Topical Application of Insulin Accelerates Vessel Maturation of Wounds by Regulating Angiopoietin-1 in Diabetic Mice. *The International Journal of Lower Extremity Wounds*. **14**(4), pp. 353-364.

Lin, X., Koelsch, G., Wu, S., Downs, D., Dashti, A., & Tang, J. (2000). Human aspartic protease memapsin 2 cleaves the β-secretase site of β-amyloid precursor protein. *Proceedings of the National Academy of Sciences of the United States of America*. **97**(4), pp. 1456-1460.

Lobov, I. B., Renard, R. A., Papadopoulos, N., Gale, N. W., Thurston, G., Yancopoulos, G. D., & Wiegand, S. J. (2007). Delta-like ligand 4 (Dll4) is induced by VEGF as a negative regulator of angiogenic sprouting. *Proceedings of the National Academy of Sciences of the United States of America*. **104**(9), pp. 3219–3224.

Luo, Y., Bolon, B., Damore, M. A., Fitzpatrick, D., Liu, H., Zhang, J., Yan, Q., Vassar, R., & Citron, M. (2003). BACE1 (β-secretase) knockout mice do not acquire compensatory gene expression changes or develop neural lesions over time. *Neurobiology of Disease*. **14**(1), pp. 81-88.

Martins-Mendes, D., Monteiro-Soares, M., Boyko, E. J., Ribeiro, M., Barata, P., Lima, J., & Soares, R. (2014). The independent contribution of diabetic foot ulcer on lower extremity amputation and mortality risk. *Journal of Diabetes and Its Complications*. **28**(5), pp. 632–638.

Matsumoto, T., & Claesson-Welsh, L. (2001). VEGF receptor signal transduction. *In Science's STKE: signal transduction knowledge environment.* **2001**(112), pp. 1945-0877.

McGinn, S., Poronnik, P., King, M., Gallery, E. D. M., & Pollock, C. A. (2003). High glucose and endothelial cell growth: Novel effects independent of autocrine TGF-β1 and hyperosmolarity. *American Journal of Physiology - Cell Physiology*. **284**(6), pp. C1374-C1386.

Meakin, P. J., Coull, B. M., Tuharska, Z., McCaffery, C., Akoumianakis, I., Antoniades, C., Brown, J., Griffin, K. J., Platt, F., Ozber, C. H., Yuldasheva, N. Y., Makava, N., Skromna, A., Prescott, A. R., McNeilly, A. D., Siddiqui, M. K., Palmer, C. N. A., Khan, F., & Ashford, M. L. (2020). Elevated circulating amyloid concentrations in obesity and diabetes promote vascular dysfunction. *Journal of Clinical Investigation*. **130**(8), pp. 4104-4117.

Meakin, P. J., Hamilton, A., Jalicy, S. M., Khan, F., & Ashford, M. L. J. (2015). BACE1 activity as a determining factor in atherosclerosis development? *Atherosclerosis*. **241**(1). pp. E13.

Meakin, P. J., Mezzapesa, A., Benabou, E., Haas, M. E., Bonardo, B., Grino, M., Brunel, J.-M., Desbois-Mouthon, C., Biddinger, S. B., Govers, R., Ashford, M. L. J., & Peiretti, F. (2018). The beta secretase BACE1 regulates the expression of insulin receptor in the liver. *Nature Communications*. **9**(1), pp. 1306.

Mehan, S., Meena, H., Sharma, D., & Sankhla, R. (2011). JNK: A stress-activated protein kinase therapeutic strategies and involvement in Alzheimer's and various neurodegenerative abnormalities. *Journal of Molecular Neuroscience*. **43**, pp. 376–390.

Michaels, J., Churgin, S. S., Blechman, K. M., Greives, M. R., Aarabi, S., Galiano, R. D., & Gurtner, G. C. (2007). db/db mice exhibit severe wound-healing impairments compared with other murine diabetic strains in a silicone-splinted excisional wound model. *Wound Repair and Regeneration*. **15**(5), pp. 665-670.

Mirza, R., & Koh, T. J. (2011). Dysregulation of monocyte/macrophage phenotype in wounds of diabetic mice. *Cytokine*. **56**(2), pp. 256-264.

Muniyappa, R., Montagnani, M., Koh, K. K., & Quon, M. J. (2007). Cardiovascular actions of insulin. *Endocrine Reviews*. **28**(5), pp. 463–491.

Murphy, H. C. (1991). The Use of Whole Animals Versus Isolated Organs or Cell Culture in Research. *Transactions of the Nebraska Academy of Sciences*. **156**, pp. 105-108.

Nakatsu, M. N., Davis, J., & Hughes, C. C. W. (2007). Optimized fibrin gel bead assay for the study of angiogenesis. *Journal of Visualized Experiments: JoVE*. **3**, pp. 186.

Nandy, D., Mukhopadhyay, D., & Basu, A. (2010). Both vascular endothelial growth factor and soluble Flt-1 are increased in type 2 diabetes but not in impaired fasting glucose. *Journal of Investigative Medicine: The Official Publication of the American Federation for Clinical Research*. **58**(6), pp. 804–806.

Neve, A., Cantatore, F. P., Maruotti, N., Corrado, A., & Ribatti, D. (2014). Extracellular matrix modulates angiogenesis in physiological and pathological conditions. *BioMed Research International*. **2014**, pp. 756078.

Ngo, D. T. M., Farb, M. G., Kikuchi, R., Karki, S., Tiwari, S., Bigornia, S. J., Bates, D. O., LaValley, M. P., Hamburg, N. M., Vita, J. A., Hess, D. T., Walsh, K., & Gokce, N. (2014). Antiangiogenic actions of vascular endothelial growth factor-A165b, an inhibitory isoform of vascular endothelial growth factor-A, in human obesity. *Circulation*. **130**(13), pp. 1072-1080.

Nichols, J. T., Miyamoto, A., Olsen, S. L., D'Souza, B., Yao, C., & Weinmaster, G. (2007). DSL ligand endocytosis physically dissociates Notch1 heterodimers before activating proteolysis can occur. *The Journal of Cell Biology*. **176**(4), pp. 445-458.

Niiyama, H., Huang, N. F., Rollins, M. D., & Cooke, J. P. (2009). Murine model of hindlimb ischemia. *Journal of Visualized Experiments*. **23**, pp. e1035.

Obata, T., Yokota, I., Yokoyama, K., Okamoto, E., Kanezaki, Y., Tanaka, Y., Maegawa, H., Teshigawara, K., Hirota, F., Yuasa, T., Kishi, K., Hattori, A., Hashida, S., Masuda, K., Matsumoto, M., Matsumoto, T., Kashiwagi, A., & Ebina, Y. (2007). Soluble insulin receptor ectodomain is elevated in the plasma of patients with diabetes. *Diabetes*. **56**, pp. 2028-2035.

Oh, H., Takagi, H., Suzuma, K., Otani, A., Matsumura, M., & Honda, Y. (1999). Hypoxia and vascular endothelial growth factor selectively up regulate angiopoietin-2 in bovine microvascular endothelial cell. *Journal of Biological Chemistry*. **274**, pp. 15732-15739.

Okonkwo, U. A., & DiPietro, L. A. (2017). Diabetes and Wound Angiogenesis. *International Journal of Molecular Sciences*. **18**(7), pp. 1419.

Ouriel, K. (2001). Peripheral arterial disease. *The Lancet*. **358**(9289), pp. 1257-1264.

Patel, S., Srivastava, S., Singh, M. R., & Singh, D. (2019). Mechanistic insight into diabetic wounds: Pathogenesis, molecular targets and treatment strategies to pace wound healing. *Biomedicine & Pharmacotherapy*. **112**, pp. 108615.

Pecoraro, R. E., Reiber, G. E., & Burgess, E. M. (1990). Pathways to diabetic limb amputation. Basis for prevention. *Diabetes Care*. **13**(5), pp. 513-521.

Pedrosa, A. R., Trindade, A., Fernandes, A. C., Carvalho, C., Gigante, J., Tavares, A. T., Diéguez-Hurtado, R., Yagita, H., Adams, R. H., & Duarte, A. (2015). Endothelial jagged1 antagonizes Dll4

regulation of endothelial branching and promotes vascular maturation downstream of Dll4/Notch1. *Arteriosclerosis, Thrombosis, and Vascular Biology*. **2015**(35), pp. 1134–1146.

Pelullo, M., Quaranta, R., Talora, C., Checquolo, S., Cialfi, S., Felli, M. P., te Kronnie, G., Borga, C., Besharat, Z. M., Palermo, R., Di Marcotullio, L., Capobianco, A. J., Gulino, A., Screpanti, I., & Bellavia, D. (2014). Notch3/Jagged1 circuitry reinforces notch signaling and sustains T-ALL. *Neoplasia*. 16(12), pp. 1007-1017.

Pendsey, S. P. (2010). Understanding diabetic foot. *International Journal of Diabetes in Developing Countries*. **30**(2), pp. 75–79.

Perez-Favila, A., Martinez-Fierro, M. L., Rodriguez-Lazalde, J. G., Cid-Baez, M. A., Zamudio-Osuna, M. de J., Martinez-Blanco, M. D. R., Mollinedo-Montaño, F. E., Rodriguez-Sanchez, I. P., Castañeda-Miranda, R., & Garza-Veloz, I. (2019). Current Therapeutic Strategies in Diabetic Foot Ulcers. *Medicina*. **55**(11), pp. 714.

Pittman, R. N. (2011). Regulation of Tissue Oxygenation. Colloquium Series on Integrated Systems *Physiology: From Molecule to Function*. **3**(3), pp. 1-100.

Pitulescu, M. E., Schmidt, I., Benedito, R., & Adams, R. H. (2010). Inducible gene targeting in the neonatal vasculature and analysis of retinal angiogenesis in mice. *Nature Protocols*. **5**, pp. 1518–1534.

Potente, M., & Carmeliet, P. (2017). The Link Between Angiogenesis and Endothelial Metabolism. *Annual Review of Physiology*. **79**(1), pp. 43-66.

Raica, M., & Cimpean, A. M. (2010). Platelet-Derived Growth Factor (PDGF)/PDGF Receptors (PDGFR) Axis as Target for Antitumor and Antiangiogenic Therapy. *Pharmaceuticals*. **3**(3), pp. 572-599.

Ramasamy, R., Yan, S. F., & Schmidt, A. M. (2011). Receptor for AGE (RAGE): signaling mechanisms in the pathogenesis of diabetes and its complications. *Annals of the New York Academy of Sciences*. **1243**(1), pp. 88-102.

Reekers, J. A., & Lammer, J. (2012). Diabetic foot and PAD: The endovascular approach. *Diabetes/Metabolism Research and Reviews*. **28**(1), pp. 36-39.

Risau, W. (1997). Mechanisms of angiogenesis. *Nature*. **386**(6626), pp. 671-674.

Roca, C., & Adams, R. H. (2007). Regulation of vascular morphogenesis by Notch signalling. *Genes and Development*. **21**, pp. 2511-2524.

Rüegg, C., Yilmaz, A., Bieler, G., Bamat, J., Chaubert, P., & Lejeune, F. J. (1998). Evidence for the involvement of endotheliai cell integrin αVβ3 in the disruption of the tumor vascuiature induced by TNF and IFN-γ. *Nature Medicine*. **4**(4), pp. 408-414.

Rust, R., Grönnert, L., Dogançay, B., & Schwab, M. E. (2019). A Revised View on Growth and Remodeling in the Retinal Vasculature. *Scientific Reports*. **9**(1), pp. 3263.

Saeedi, P., Petersohn, I., Salpea, P., Malanda, B., Karuranga, S., Unwin, N., Colagiuri, S., Guariguata, L., Motala, A. A., Ogurtsova, K., Shaw, J. E., Bright, D., & Williams, R. (2019). Global and regional diabetes prevalence estimates for 2019 and projections for 2030 and 2045: Results from the International Diabetes Federation Diabetes Atlas, 9th edition. *Diabetes Research and Clinical Practice*. **157**, pp. 107843.

Sathya, M., Premkumar, P., Karthick, C., Moorthi, P., Jayachandran, K. S., & Anusuyadevi, M. (2012). BACE1 in Alzheimer's disease. *Clinica Chimica Acta*. **24**(414), pp. 171-8.

Sawada, N., & Arany, Z. (2017). Metabolic regulation of angiogenesis in diabetes and aging. In Physiology. **32**(4), pp. 290-307.

Seitz, O., Schürmann, C., Hermes, N., Müller, E., Pfeilschifter, J., Frank, S., & Goren, I. (2010). Wound healing in mice with high-fat diet- or ob gene-induced diabetes-obesity syndromes: a comparative study. *Experimental Diabetes Research*. **2010**, pp. 476969.

Shalaby, F., Janet, R., Yamaguchi, T. P., Gertsenstein, M., Wu, X. F., Breitman, M. L., & Schuh, A. C. (1995). Failure of blood-island formation and vasculogenesis in Flk-1-deficient mice. *Nature*. **376**, pp. 62-66.

Shepro, D., & Morel, N. M. (1993). Pericyte physiology. *The FASEB Journal*. **7**(11), pp. 1031-1038.

Shibuya, M. (2011). Vascular Endothelial Growth Factor (VEGF) and Its Receptor (VEGFR) Signaling in Angiogenesis: A Crucial Target for Anti- and Pro-Angiogenic Therapies. *Genes and Cancer*. **2**(12), pp. 1097-1105.

Shimizu, H., Tosaki, A., Kaneko, K., Hisano, T., Sakurai, T., & Nukina, N. (2008). Crystal structure of an active form of BACE1, an enzyme responsible for amyloid beta protein production. *Molecular and Cellular Biology*. **28**(11), pp. 3663-3671.

Siemerink, M. J., Klaassen, I., van Noorden, C. J. F., & Schlingemann, R. O. (2013). Endothelial Tip Cells in Ocular Angiogenesis: Potential Target for Anti-Angiogenesis Therapy. *Journal of Histochemistry and Cytochemistry*. **61**(2), pp. 101–115.

Sinha, S., Anderson, J. P., Barbour, R., Basi, G. S., Caccavello, R., Davis, D., Doan, M., Dovey, H. F., Frigon, N., Hong, J., Jacobson-Croak, K., Jewett, N., Keim, P., Knops, J., Lieberburg, I., Power, M., Tan, H., Tatsuno, G., Tung, J., … John, V. (1999). Purification and cloning of amyloid precursor protein β-secretase from human brain. *Nature*. **402**(6761), pp. 537-540.

Stapor, P., Wang, X., Goveia, J., Moens, S., & Carmeliet, P. (2014). Angiogenesis revisited - Role and therapeutic potential of targeting endothelial metabolism. *Journal of Cell Science*. **127**, pp. 4331-4341.

Staton, C. A., Reed, M. W. R., & Brown, N. J. (2009). A critical analysis of current *in vitro* and *in vivo* angiogenesis assays. *International Journal of Experimental Pathology*. **90**, pp. 195-221

Stern, D. M., Yan, S. Du, Yan, S. F., & Schmidt, A. M. (2002). Receptor for advanced glycation endproducts (RAGE) and the complications of diabetes. *Ageing Research Reviews*. **1**(1), pp. 1-15.

Stockley, J. H., & O'Neill, C. (2008). Understanding BACE1: Essential protease for amyloid-β production in Alzheimer's disease. *Cellular and Molecular Life Sciences*. **65**, pp. 3265.

Suchting, S., & Eichmann, A. (2009). Jagged Gives Endothelial Tip Cells an Edge. *Cell*. **137**(6), pp. 988-990.

Swift, M. R., & Weinstein, B. M. (2009). Arterial-venous specification during development. *Circulation Research*. **104**, pp. 576-588.

Tamagno, E., Guglielmotto, M., Aragno, M., Borghi, R., Autelli, R., Giliberto, L., Muraca, G., Danni, O., Zhu, X., Smith, M. A., Perry, G., Jo, D.-G., Mattson, M. P., & Tabaton, M. (2008). Oxidative stress

activates a positive feedback between the γ- and β-secretase cleavages of the β-amyloid precursor protein. *Journal of Neurochemistry*. **104**(3), pp. 683-695.

Tan, S. Y., Mei Wong, J. L., Sim, Y. J., Wong, S. S., Mohamed Elhassan, S. A., Tan, S. H., Ling Lim, G. P., Rong Tay, N. W., Annan, N. C., Bhattamisra, S. K., & Candasamy, M. (2019). Type 1 and 2 diabetes mellitus: A review on current treatment approach and gene therapy as potential intervention. *Diabetes & Metabolic Syndrome: Clinical Research & Reviews*. **13**(1), pp. 364-372.

Thalgott, J. H., Dos-Santos-Luis, D., Hosman, A. E., Martin, S., Lamandé, N., Bracquart, D., Srun, S., Galaris, G., de Boer, H. C., Tual-Chalot, S., Kroon, S., Arthur, H. M., Cao, Y., Snijder, R. J., Disch, F., Mager, J. J., Rabelink, T. J., Mummery, C. L., Raymond, K., & Lebrin, F. (2018). Decreased Expression of Vascular Endothelial Growth Factor Receptor 1 Contributes to the Pathogenesis of Hereditary Hemorrhagic Telangiectasia Type 2. *Circulation*. **138**(23), pp. 2698-2712.

Thiruvoipati, T., Kielhorn, C. E., & Armstrong, E. J. (2015). Peripheral artery disease in patients with diabetes: Epidemiology, mechanisms, and outcomes. *World Journal of Diabete*s. **6**(7), pp. 961-969.

Turner, R. T. 3rd, Hong, L., Koelsch, G., Ghosh, A. K., & Tang, J. (2005). Structural locations and functional roles of new subsites S5, S6, and S7 in memapsin 2 (beta-secretase). *Biochemistry*. **44**(1), pp. 105-112.

Ushio-Fukai, M., Tang, Y., Fukai, T., Dikalov, S. I., Ma, Y., Fujimoto, M., Quinn, M. T., Pagano, P. J., Johnson, C., & Alexander, R. W. (2002). Novel role of gp91phox-containing NAD(P)H oxidase in vascular endothelial growth factor-induced signaling and angiogenesis. *Circulation Research*. **91**(12), pp. 1160–1167.

Vailhé, B., Vittet, D., & Feige, J. J. (2001). In vitro models of vasculogenesis and angiogenesis. In Laboratory Investigation. **81**, pp. 439-452.

Vassar, R., Bennett, B. D., Babu-Khan, S., Kahn, S., Mendiaz, E. A., Denis, P., Teplow, D. B., Ross, S., Amarante, P., Loeloff, R., Luo, Y., Fisher, S., Fuller, J., Edenson, S., Lile, J., Jarosinski, M. A., Biere, A. L., Curran, E., Burgess, T., … Citron, M. (1999). β-Secretase cleavage of Alzheimer's amyloid precursor protein by the transmembrane aspartic protease BACE. *Science*. **286**(5440), pp. 735-741.

Vassar, R., Kovacs, D. M., Yan, R., & Wong, P. C. (2009). The β-secretase enzyme BACE in health and Alzheimer's disease: Regulation, cell biology, function, and therapeutic potential. *Journal of Neuroscience*. **29**(41), pp. 12787-12794.

Volpe, C. M. O., Villar-Delfino, P. H., Dos Anjos, P. M. F., & Nogueira-Machado, J. A. (2018). Cellular death, reactive oxygen species (ROS) and diabetic complications. *Cell Death & Disease*. **9**(2), pp. 119.

Wen, Y., Yu, W. H., Maloney, B., Bailey, J., Ma, J., Marié, I., Maurin, T., Wang, L., Figueroa, H., Herman, M., Krishnamurthy, P., Liu, L., Planel, E., Lau, L.-F., Lahiri, D. K., & Duff, K. (2008). Transcriptional regulation of beta-secretase by p25/cdk5 leads to enhanced amyloidogenic processing. *Neuron*. **57**(5), pp. 680-690.

Wietecha, M. S., Chen, L., Ranzer, M. J., Anderson, K., Ying, C., Patel, T. B., & DiPietro, L. A. (2011). Sprouty2 downregulates angiogenesis during mouse skin wound healing. American Journal of Physiology. *Heart and Circulatory Physiology*. **300**(2), pp. H459-H467.

Wilcox, G. (2005). Insulin and insulin resistance. *The Clinical Biochemist. Reviews*. **26**(2), pp. 19-39.

Woolard, J., Bevan, H. S., Harper, S. J., & Bates, D. O. (2009). Molecular diversity of VEGF-A as a regulator of its biological activity. *Microcirculation*. **16**(7), pp. 572-592.

Xu, Y., Li, M. J., Greenblatt, H., Chen, W., Paz, A., Dym, O., Peleg, Y., Chen, T., Shen, X., He, J., Jiang, H., Silman, I., & Sussman, J. L. (2012). Flexibility of the flap in the active site of BACE1 as revealed by crystal structures and molecular dynamics simulations. *Acta Crystallographica Section D: Biological Crystallography*. **68**, pp. 13-25.

Yamagishi, S., Kawakami, T., Fujimori, H., Yonekura, H., Tanaka, N., Yamamoto, Y., Urayama, H., Watanabe, Y., & Yamamoto, H. (1999). Insulin stimulates the growth and tube formation of human microvascular endothelial cells through autocrine vascular endothelial growth factor. *Microvascular Research*. **57**(3), pp. 329-339.

Yan, R., Blenkowski, M. J., Shuck, M. E., Miao, H., Tory, M. C., Pauley, A. M., Brashler, J. R., Stratman, N. C., Mathews, W. R., Buhl, A. E., Carter, D. B., Tomasselll, A. G., Parodl, L. A., Helnrikson, R. L., & Gurney, M. E. (1999). Membrane-anchored aspartyl protease with Alzheimer's disease β- secretase activity. *Nature*. **402**, pp. 533–537.

Yan, R., Han, P., Miao, H., Greengard, P., & Xu, H. (2001). The Transmembrane Domain of the Alzheimer's β-Secretase (BACE1) Determines its Late Golgi Localization and Access to β-Amyloid Precursor Protein (APP) Substrate. *Journal of Biological Chemistry*. **276**, pp. 36788-36796.

Yan, X., Chen, B., Lin, Y., Li, Y., Xiao, Z., Hou, X., Tan, Q., & Dai, J. (2010). Acceleration of diabetic wound healing by collagen-binding vascular endothelial growth factor in diabetic rat model. *Diabetes Research and Clinical Practice*. **90**(1), pp. 66-72.

Zhang, X., Zhou, K., Wang, R., Cui, J., Lipton, S. A., Liao, F.-F., Xu, H., & Zhang, Y. (2007). Hypoxia-inducible factor 1alpha (HIF-1alpha)-mediated hypoxia increases BACE1 expression and beta-amyloid generation. *The Journal of Biological Chemistry*. **282**(15), pp. 10873-10880.

Zheng, X., Narayanan, S., Sunkari, V. G., Eliasson, S., Botusan, I. R., Grünler, J., Catrina, A. I., Radtke, F., Xu, C., Zhao, A., Ekberg, N. R., Lendahl, U., & Catrina, S. B. (2019). Triggering of a Dll4–Notch1 loop impairs wound healing in diabetes. *Proceedings of the National Academy of Sciences of the United States of America*. **116**(14), pp. 6985-6994.

Ziche, M., & Morbidelli, L. (2000). Nitric Oxide and Angiogenesis. *Journal of Neuro-Oncology*. **50**(1), pp. 139-148.

Ziche, M., Morbidelli, L., Masini, E., Amerini, S., Granger, H. J., Maggi, C. A., Geppetti, P., & Ledda, F. (1994). Nitric oxide mediates angiogenesis *in vivo* and endothelial cell growth and migration *in vitro* promoted by substance P. *The Journal of Clinical Investigation*. **94**(5), pp. 2036–2044.

Zuazo-Gaztelu, I., & Casanovas, O. (2018). Unraveling the role of angiogenesis in cancer ecosystems. *Frontiers in Oncology*. **8**, pp. 248.

5.1 Websites consulted

APMA. 2020. *Diabetic Wound Care*. [Online]. [Accessed 10th July 2020]. Available from: https://www.apma.org/diabeticwoundcare.

International Diabetes Federation. 2019. [Online]. *IDF Diabetes Atlas 9th Edition*. [Accessed 22nd April 2020]. Available from: http://www.idf.org/diabetesatlas.

National Institute for Health and Care Excellence. 2013. [Online]. *Diabetic foot problems: prevention and management (NG19).* [Accessed 23rd May 2020]. Available from: https://www.nice.org.uk/guidance/ng19.

Sigma-Aldrich. 2020. [Online]. *β-Secretase Inhibitor IV - CAS 797035-11-1 – Calbiochem*. [Accessed 15th July 2020]. Available from: https://www.sigmaaldrich.com/catalog/product/mm/565788?lang=en&region=GB